Hidden SU(2) symmetries, the symmetry hierarchy, and the emergent eightfold way in spin-1 quantum magnets

Hui-Ke Jin,[1] Jian-Jian Miao,[2] and Yi Zhou[1,3,4,5]

[1]Department of Physics, Zhejiang University, Hangzhou 310027, China
[2]Kavli Institute for Theoretical Sciences, University of Chinese Academy of Sciences, Beijing 100190, China
[3]Beijing National Laboratory for Condensed Matter Physics & Institute of Physics, Chinese Academy of Sciences, Beijing 100190, China
[4]CAS Center for Excellence in Topological Quantum Computation, University of Chinese Academy of Sciences, Beijing 100190, China
[5]Collaborative Innovation Center of Advanced Microstructures, Nanjing University, Nanjing 210093, China

(Received 3 January 2019; published 1 August 2019)

The largest allowed symmetry in a spin-1 quantum system is an SU(3) symmetry rather than the SO(3) spin rotation. In this work, we reveal some SU(2) symmetries as subgroups of SU(3) that, to the best of our knowledge, have not previously been recognized. Then, we construct SU(2) symmetric Hamiltonians and explore the ground-state phase diagram in accordance with the SU(3) $\supset$ SU(2) $\times$ $U(1)$ symmetry hierarchy. It is natural to treat the eight generators of the SU(3) symmetry on an equal footing; this approach is called the eightfold way. We find that the spin spectral functions and spin quadrupole spectral functions share the same structure, provided that the elementary excitations are flavor waves at low energies, which serves as a clue to the eightfold way. An emergent $S = 1/2$ quantum spin liquid is proposed to coexist with gapful spin nematic order in one of the ground states. In analogy to quantum chromodynamics, we find the gap relation for hydrodynamic modes in quantum spin-orbital liquid states, which is nothing but the Gell-Mann-Okubo formula.

DOI: 10.1103/PhysRevB.100.085101

I. INTRODUCTION

The symmetry principle plays a fundamental role with respect to the laws of nature. It provides an infrastructure and coherence for summarizing physical laws that are independent of any specific dynamics. Noether's theorem says that every continuous symmetry of the action of a physical system is associated with a corresponding conservation law. The standard paradigm for describing phase transitions and critical phenomena is Landau's theory of symmetry breaking. The states of matter are classified on the basis of symmetries. A higher-temperature phase is of a high symmetry characterized by a group G, while a lower-temperature phase is of a low symmetry characterized by a subgroup $H \subset G$. A low-energy effective theory can be constructed in terms of order parameters and is described by all terms that are allowed according to the relevant symmetries. A hierarchy of symmetries is also widely used in particle physics to understand the dynamics of elementary particles.

Meanwhile, spin-1 quantum magnets are of great interest in physics. One famous example is the Haldane phase in one-dimensional (1D) spin-1 chains [1], in which fractional spin-1/2 end states are protected by the spin rotational symmetry in a phenomenon called symmetry-protected topological order [2–5]. Spin-1 systems are also able to host spin nematic orders in dimensions of $D > 1$; such orders are characterized by long-range spin quadrupolar correlations, and the possibility for fractional spinon excitations to coexist with spin nematic orders has also been proposed [6]. Such quantum magnets are widely encountered in various materials, especially transition metal compounds, in which a local $S = 1$ magnetic moment can be formed in a cation via Hund's coupling; examples include $3d^8$ Ni^{2+} and $3d^6$ Fe^{2+}. In this work, we shall reveal several hidden SU(2) symmetries in spin-1 quantum magnets in addition to spin rotational symmetry, and we will study spin-1 quantum systems with the help of the symmetry hierarchy.

For a spin-1 quantum magnet, there are three local states, namely, $|S^z = \pm 1\rangle$ and $|S^z = 0\rangle$, and eight independent local Hermitian operators: three spin vector operators, S^x, S^y, and S^z, and five spin quadrupolar operators:

$$\begin{aligned} Q^{x^2-y^2} &= (S^x)^2 - (S^y)^2, \\ Q^{3z^2-r^2} &= \frac{1}{\sqrt{3}}[2(S^z)^2 - (S^x)^2 - (S^y)^2], \\ Q^{xy} &= S^xS^y + S^yS^x, \\ Q^{yz} &= S^yS^z + S^zS^y, \\ Q^{zx} &= S^zS^x + S^xS^z. \end{aligned} \tag{1}$$

To illustrate the symmetry hierarchy, we consider a generic two-body interacting Hamiltonian as follows:

$$\mathcal{H} = \sum_{\langle i,j\rangle}\left(\sum_{\alpha\beta} J_{\alpha\beta}S_i^\alpha S_j^\beta + \sum_{\mu\nu} J_{\mu\nu}Q_i^\mu Q_j^\nu + \sum_{\alpha\mu} I_{\alpha\mu}S_i^\alpha Q_j^\mu\right), \tag{2}$$

where $\langle i,j\rangle$ is a pair of nearest neighboring sites; α and β denote x, y, and z; and μ and ν denote x^2-y^2, $3z^2-r^2$, xy, yz, and zx. The SO(3) spin rotational symmetry is achieved when $I_{\alpha\mu} = 0$, $J_{\alpha\beta} = \delta_{\alpha\beta}J_1$, and $J_{\mu\nu} = \delta_{\mu\nu}J_2$. Furthermore, $\mathcal{H}$ will be SU(3) symmetric when $J_1 = J_2$, and the SU(3) group is generated by eight operators $\{\boldsymbol{S}, \boldsymbol{Q}\}$ [7–9].

The SO(3) model is well studied: a phase diagram consisting of a ferromagnetic phase, a dimerized phase, Haldane phases and a critical phase has been constructed in one dimension [10–13], and the SO(3) model can host spin nematic ground states in dimensions of $D > 1$ [6,14–21].

The model defined in Eq. (2) has typically been studied in accordance with the $SU(3) \supset SO(3) \cdots$ symmetry hierarchy. Nevertheless, there are other SU(2) subgroups belonging to the SU(3) group, and this fact implies the existence of a slice of SU(2) symmetries in addition to the SO(3) spin rotation in spin-1 quantum magnets of which, to the best of our knowledge, the research community is not aware. This situation inspires us to search for Hamiltonians that respect these hidden symmetries; for this purpose, a new symmetry hierarchy, $SU(3) \supset SU(2) \times U(1) \cdots$, will be adopted to reveal novel states with various low-energy excitations. To describe these states, it is natural to treat all operators $\{\boldsymbol{S}, \boldsymbol{Q}\}$ on an equal footing, which is reminiscent of the "eightfold way" in quantum chromodynamics (QCD).

The paper is organized as follows. We reveal hidden SU(2) symmetries and construct corresponding SU(2) symmetric Hamiltonians in Sec. II. In the spirit of eightfold way, we apply flavor-wave mean-field theory to study the $SU(2) \times U(1)$ model and demonstrate that the similar structure in spin spectral functions and spin quadrupole spectral functions serves a clue to the eightfold way in Sec. III. In Sec. IV, we go beyond the mean-field theory and find an emergent $S = 1/2$ gapless quantum spin liquid state coexisting with spin nematic order. We also find Gell-Mann-Okubo formula like gap relations for the hydrodynamic modes in quantum spin-orbital liquid states. Section V is devoted to summary.

II. HIDDEN SU(2) SYMMETRIES AND HAMILTONIANS

A. Hidden SU(2) symmetries

It turns out that there are three hidden SU(2) symmetries in addition to well known spin rotational SO(3) symmetry in a spin-1 system, which are generated as follows (see Appendix B):

$$\begin{aligned} SU(2)_\alpha &: \left\{Q^{zx}, S^y, \frac{1}{2}Q^{x^2-y^2} + \frac{\sqrt{3}}{2}Q^{3z^2-r^2}\right\}, \\ SU(2)_\beta &: \left\{Q^{yz}, S^x, \frac{1}{2}Q^{x^2-y^2} - \frac{\sqrt{3}}{2}Q^{3z^2-r^2}\right\}, \\ SU(2)_\gamma &: \{Q^{xy}, S^z, Q^{x^2-y^2}\}. \end{aligned} \tag{3}$$

Each set of these generators consists of one component of the spin vector $\boldsymbol{S}$ and two components of the spin quadrupole $\boldsymbol{Q}$. Note that these three sets of generators are related to each other by the following cycle: $S^x \to S^y \to S^z \to S^x$. In the remaining part of this work, we shall focus on $SU(2)_\gamma$; $SU(2)_\alpha$ and $SU(2)_\beta$ can then be obtained in accordance with this cycle.

For the $SU(2)_\gamma$ symmetry, S^z generates spin rotations along the z axis, and the other two generators, Q^{xy} and $Q^{x^2-y^2}$, correspond to *two-magnon* processes, as can be seen from

$$Q^{x^2-y^2} = \frac{1}{2}[(S^+)^2 + (S^-)^2], \tag{4a}$$

$$Q^{xy} = \frac{1}{2i}[(S^+)^2 - (S^-)^2], \tag{4b}$$

where $S^\pm = S^x \pm iS^y$. Let us define

$$J^z = \tfrac{1}{2}S^z, \tag{5a}$$

$$J^+ = \tfrac{1}{2}\left(Q^{x^2-y^2} + iQ^{xy}\right) = \tfrac{1}{2}(S^+)^2, \tag{5b}$$

$$J^- = \tfrac{1}{2}\left(Q^{x^2-y^2} - iQ^{xy}\right) = \tfrac{1}{2}(S^-)^2. \tag{5c}$$

It is easy to verify that $\{J^z, J^\pm\}$ satisfy the SU(2) Lie algebra. Therefore the spontaneous breaking of the $SU(2)_\gamma$ symmetry along the S^z direction will give rise to *two-magnon* low-energy excitations, while spontaneous symmetry breaking along the Q^{xy} and $Q^{x^2-y^2}$ directions will give rise to an admixture of *one- and two-magnon* excitations, which will tend to restore the $SU(2)_\gamma$ symmetry.

The underlying SU(3) structure and the hidden SU(2) symmetries will be more transparent in the Cartesian representation of the spin states: $|x\rangle = i(|1\rangle - |-1\rangle)/\sqrt{2}$, $|y\rangle = (|1\rangle + |-1\rangle)/\sqrt{2}$, and $|z\rangle = -i|0\rangle$. Then, a spin state can be written as $|\boldsymbol{d}\rangle = d^x|x\rangle + d^y|y\rangle + d^z|z\rangle$, where $\boldsymbol{d} = (d^x, d^y, d^z)$ is a complex vector and the normalization condition is given by $|\boldsymbol{d}|^2 = 1$. The expectation values for $\{\boldsymbol{S}, \boldsymbol{Q}\}$ can be expressed in terms of $\boldsymbol{d}$ as follows:

$$\begin{aligned} \langle S^\alpha\rangle &= -i\epsilon_{\alpha\beta\gamma}\bar{d}^\beta d^\gamma, \\ \langle Q^{\alpha\beta}\rangle|_{\alpha\neq\beta} &= -(\bar{d}^\alpha d^\beta + \bar{d}^\beta d^\alpha), \\ \langle Q^{x^2-y^2}\rangle &= |d^y|^2 - |d^x|^2, \\ \langle Q^{3z^2-r^2}\rangle &= \frac{1}{\sqrt{3}}(2|d^z|^2 - |d^y|^2 - |d^x|^2), \end{aligned} \tag{6}$$

where $\bar{d}^\alpha$ is the complex conjugate of d^α and $\epsilon^{\alpha\beta\gamma}$ is a three-rank antisymmetric tensor. Thus, a spin-1 quantum system can be described by the following path integral:

$$\mathcal{Z} = \int \mathcal{D}[\boldsymbol{d}, \bar{\boldsymbol{d}}\,]\delta(|\boldsymbol{d}|^2 - 1)e^{-\int_0^\beta d\tau\{\sum_i \bar{\boldsymbol{d}}_i\cdot\partial_\tau\boldsymbol{d}_i - \mathcal{H}\}}, \tag{7}$$

where the Hamiltonian $\mathcal{H}$ is given by Eq. (2) with $\{\boldsymbol{S}, \boldsymbol{Q}\}$ replaced with their expectation values. Now, it is clear that all of the special unitary transformations of $\boldsymbol{d}$ give rise to the SU(3) group and that the special unitary transformations of any two components of $\boldsymbol{d}$ lead to either $SU(2)_\alpha$, $SU(2)_\beta$, or $SU(2)_\gamma$.

B. SU(2)-symmetric Hamiltonians

Now, we are in a position to construct Hamiltonians in accordance with the $SU(2)_\gamma$ symmetry. A generic spin-1 Hamiltonian can be written in terms of $\{\boldsymbol{S}, \boldsymbol{Q}\}$ in a bilinear form as shown in Eq. (2). Using group theory, one is able to obtain all $SU(2)_\gamma$-symmetric two-body interactions (see Appendix C). These $SU(2)_\gamma$-symmetric Hamiltonians are

TABLE I. Typical $\mathrm{SU}(2)_\gamma$-symmetric Hamiltonians in Eq. (8), which are classified with respect to time reversal ($\mathcal{T}$), spatial inversion ($\mathcal{I}$), and additional global/local symmetries.

Hamiltonian	$\mathcal{T}$	$\mathcal{I}$	Global	Local
$\mathcal{H}_1$	Yes	Yes	$\mathrm{SU}(2)\times U(1)$	$U(1)$
$\mathcal{H}_2$	Yes	Yes	$\mathrm{SU}(2)\times U(1)$	
$\mathcal{H}_3$	Yes	Yes	$\mathrm{SU}(2)\times U(1)$	$U(2)$
$\mathcal{H}_4$	Yes	No	SU(2)	
$\mathcal{H}_5$	No	No	$\mathrm{SU}(2)\times U(1)$	
$\mathcal{H}_6$	No	No	SU(2)	

linear combinations of the following six terms:

$$\mathcal{H}_1=\sum_{\langle i,j\rangle} S_i^zS_j^z+Q_i^{xy}Q_j^{xy}+Q_i^{x^2-y^2}Q_j^{x^2-y^2}, \tag{8a}$$

$$\mathcal{H}_2=\sum_{\langle i,j\rangle} S_i^xS_j^x+Q_i^{yz}Q_j^{yz}+S_i^yS_j^y+Q_i^{zx}Q_j^{zx}, \tag{8b}$$

$$\mathcal{H}_3=\sum_{\langle i,j\rangle} Q_i^{3z^2-r^2}Q_j^{3z^2-r^2}, \tag{8c}$$

$$\mathcal{H}_4=\sum_{\langle i,j\rangle} D_{ij}\big[S_i^xS_j^y+Q_i^{yz}Q_j^{zx}-(i\leftrightarrow j)\big], \tag{8d}$$

$$\mathcal{H}_5=\sum_{\langle i,j\rangle} D_{ij}\big[S_i^yQ_j^{zx}+Q_i^{yz}S_j^x-(i\leftrightarrow j)\big], \tag{8e}$$

$$\mathcal{H}_6=\sum_{\langle i,j\rangle} D_{ij}\big[Q_i^{zx}S_j^x+Q_i^{yz}S_j^y-(i\leftrightarrow j)\big], \tag{8f}$$

where the $D_{ij}=-D_{ji}=\pm1$ define a direction along each bond $\langle i,j\rangle$ and are translationally invariant. The Hamiltonians $\mathcal{H}_{1-6}$ can be classified with respect to the time-reversal symmetry $\mathcal{T}$, the spatial inversion symmetry $\mathcal{I}$, and additional symmetries as summarized in Table I.

Further discussions are presented as follows: (1) $\mathcal{H}_1$ consists of the $\mathrm{SU}(2)_\gamma$ generators $\{S_i^z,Q_i^{xy},Q_i^{x^2-y^2}\}$ and can be viewed as a spin-1/2 Heisenberg model in the subspace spanned by the local basis $\{|x\rangle_i,|y\rangle_i\}$. (2) Let us define $\Lambda_8=\sum_i Q_i^{3z^2-r^2}$; then, we have $[\Lambda_8,\mathcal{H}_1]=[\Lambda_8,\mathcal{H}_2]=[\Lambda_8,\mathcal{H}_3]=[\Lambda_8,\mathcal{H}_5]=0$. Thus, $\mathcal{H}_{1-3}$ and $\mathcal{H}_5$ have an $\mathrm{SU}(2)_\gamma\times U(1)$ symmetry, where the additional global $U(1)$ symmetry is generated by Λ_8. (3) $\mathcal{H}_1$ has an additional local $U(1)$ symmetry generated by $Q_i^{3z^2-r^2}$. (4) $\mathcal{H}_3$ has an additional local $U(2)$ symmetry that is generated by $\{S_i^z,Q_i^{xy},Q_i^{x^2-y^2}\}$ and $Q_i^{3z^2-r^2}$.

III. EIGHTFOLD WAY AND FLAVOR-WAVE MEAN-FIELD THEORY: SU(2) × $U(1)$ × $\mathcal{T}$ × $\mathcal{I}$ MODEL

Regarding the $\mathrm{SU}(3)\supset\mathrm{SU}(2)\times U(1)$ symmetry hierarchy, we would like to treat all of the SU(3) generators $\{\boldsymbol{S},\boldsymbol{Q}\}$ on an equal footing. In this spirit, we study ground states and low-energy excitations with the help of flavor-wave mean-field theory [22–25], and then discuss how the spectral functions can be exploited to detect the eightfold way.

First, we minimize the energy functional $\mathcal{H}(\boldsymbol{d},\bar{\boldsymbol{d}})$ with respect to the complex fields $\boldsymbol{d}_i$ to determine the ground state. Second, we assign three flavors of Schwinger bosons, $a_{n\alpha}(j)$, to each site j on the nth sublattice, where $\alpha=x,y,z$ refers to the local spin states. For example, $n=1$ for a uniform state, while $n=1,2$ for a bipartite-lattice ordered state. The operators $\{\boldsymbol{S},\boldsymbol{Q}\}$ can be written bilinearly in terms of the Schwinger bosons, and the physical Hilbert space can be restored by imposing a single-occupancy condition (see Appendix D). Third, without loss of generality, we let the Schwinger bosons condense at $a_{n\tilde{x}}$ to obtain ordered states, where $a_{n\tilde{x}}$ and the other two orthogonal components, $a_{n\tilde{y}}$ and $a_{n\tilde{z}}$, are related to (a_{nx},a_{ny},a_{nz}) by an SU(3) rotation Ω_n as follows: $(a_{n\tilde{x}},a_{n\tilde{y}},a_{n\tilde{z}})^T=\Omega_n(a_{nx},a_{ny},a_{nz})^T$. Such an Ω_n is determined by the mean-field vector $\boldsymbol{d}$ and enables us to attribute the condensate to $a_{n\tilde{x}}$ alone, while treating $a_{n\tilde{y}}$ and $a_{n\tilde{z}}$ as small fractions. Then, the low-energy Hamiltonian can be bilinearized by the Holstein-Primakoff transformation: $a_{n\tilde{x}}^\dagger(j)=a_{n\tilde{x}}(j)=\sqrt{M-a_{n\tilde{y}}^\dagger(j)a_{n\tilde{y}}(j)-a_{n\tilde{z}}^\dagger(j)a_{n\tilde{z}}(j)}$, where we will ultimately take $M=1$ for the single-occupancy case. Expansion in $1/M$ and Bogoliubov transformation will give rise to a diagonalized Hamiltonian in k space (see Appendix D): $\mathcal{H}=\sum_{m,\boldsymbol{k}}\omega_m(\boldsymbol{k})b_m^\dagger(\boldsymbol{k})b_m(\boldsymbol{k})+\mathcal{C}$, where $\omega_m(\boldsymbol{k})$ is the energy dispersion of the mth flavor-wave branch, $b_m(\boldsymbol{k})$ is a bosonic Bogoliubov quasiparticle, and $\mathcal{C}$ is a constant. For a uniform state, $m=1,\ 2$, while for a bipartite-lattice ordered state, $m=1,\ 2,\ 3,\ 4$. As long as the vector $\boldsymbol{d}$ is given by the mean-field theory, we will be able to obtain $\omega_m(\boldsymbol{k})$ and $b_m(\boldsymbol{k})$ simultaneously.

In particular, we are interested in Hamiltonians with the time-reversal symmetry $\mathcal{T}$ and the spatial inversion symmetry $\mathcal{I}$, which can be parameterized in terms of three real numbers $K_1,\ K_2$, and K_3 as follows:

$$\mathcal{H}=K_1\mathcal{H}_1+K_2\mathcal{H}_2+K_3\mathcal{H}_3. \tag{9}$$

Note that the model given in Eq. (9) respects the $\mathrm{SU}(2)_\gamma\times U(1)$ symmetry rather than the $\mathrm{SU}(2)_\gamma$ symmetry. For simplicity, we shall consider bipartite lattices only, including a 1D chain, a square lattice and a cubic lattice.

A. Ground states

To explore the ground-state phase diagram, we set $K_1^2+K_2^2+K_3^2=1$, such that the parameter space is a sphere. Top and bottom views (along the K_3 axis) of this sphere are displayed in Fig. 1, where the mean-field phase diagram is presented. There are six ordered phases, FQ1, FQ2, FQ3, AFQ1, AFQ2, and AFQ3. Here, FQ refers to a ferroquadrupolar state, and AFQ refers to an antiferro-quadrupolar state (or, to be precise, a state with a staggered quadrupolar order). When $K_{1(2,3)}$ is negative and predominates, the ground states are FQ states, while when $K_{1(2,3)}$ is positive and predominates, the ground states are AFQ states. The solid lines in the phase diagram represent first-order transitions, while the dashed lines represent continuous transitions. The SU(3) symmetry will be achieved at two points where $K_1=K_2=K_3$. Both SU(3) points are tricritical points. The one with $K_{1,2,3}<0$ corresponds to three phases, FQ1, FQ2, and FQ3, while the

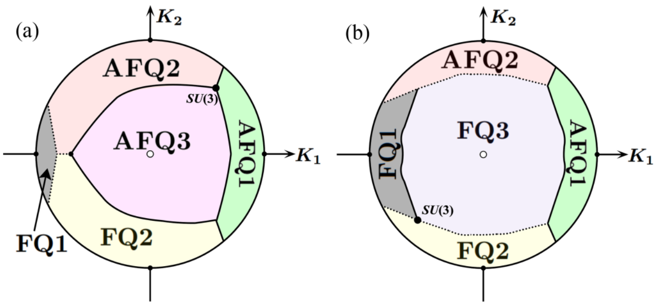

FIG. 1. Mean-field phase diagrams for $\mathrm{SU}(2)\times U(1)\times\mathcal{T}\times\mathcal{I}$-symmetric models as defined in Eq. (9) on bipartite lattices. Two SU(3) points are located at $K_1=K_2=K_3$. (a) Top view of the parameter space ($K_3>0$). (b) Bottom view of the parameter space ($K_3<0$). Solid lines indicate first-order phase transitions, while dashed lines indicate continuous transitions.

other one, with $K_{1,2,3}>0$, corresponds to AFQ1, AFQ2, and AFQ3.

We use local spin density to illustrate the wave functions for various FQ and AFQ states. If $\boldsymbol{d}$ vector is real, the state is time-reversal invariant, and the local spin density $|\langle\hat{S}(\hat{n})|\boldsymbol{d}\rangle|^2$ is invariant under an SO(2) rotation along the axis of $(|d_x|,|d_y|,|d_z|)$, which is so-called SO(2) symmetric pattern. Otherwise, $|\boldsymbol{d}\rangle$ breaks the time-reversal symmetry, $|\langle\hat{S}(\hat{n})|\boldsymbol{d}\rangle|^2$ will be distorted from an SO(2) symmetric pattern to an SO(2) nonsymmetric pattern. Two examples for time-reversal invariant state and time-reversal breaking state are given in Fig. 2

All the six quadrupolar ordered states are illustrated on square lattice in Fig. 3, where we choose time-reversal invariant ground states to eliminate spin dipolar orders and manifest quadrupolar orders. Notably, dipolar and quadrupolar orders may coexist in a ground state in the FQ1, FQ2, AFQ1, and AFQ2 phases, while only a quadrupolar order exists in the FQ3 and AFQ3 phases.

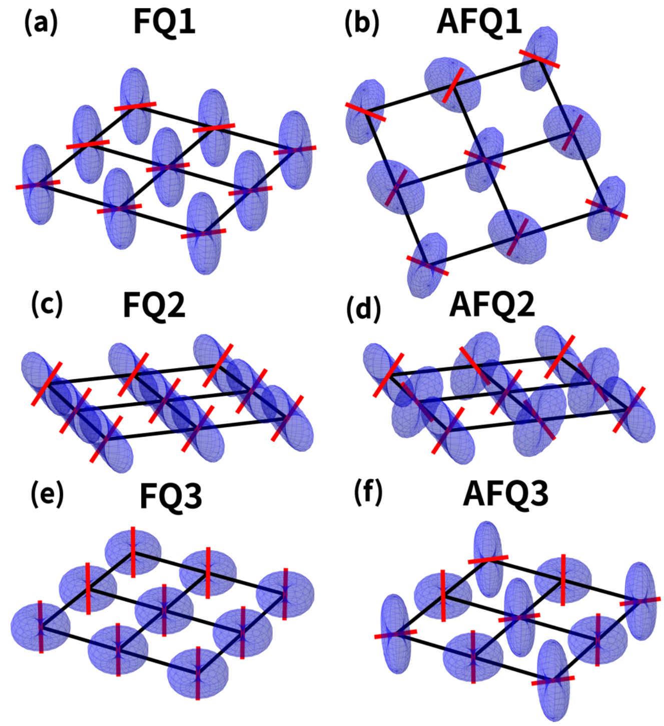

FIG. 3. Six types of spin quadrupolar orders on square lattice. All the states are time-reversal invariant with real $\boldsymbol{d}$ vectors, and red bars indicate the directions of these real $\boldsymbol{d}$ vectors. Blue surfaces represent the spin density of a local wave function Ψ, which is defined as $|\langle\hat{S}(\hat{n})|\Psi\rangle|^2$. Here, $|\hat{S}(\hat{n})\rangle$ is the spin coherent state pointing along direction $\hat{n}$ and is defined by $(\hat{n}\cdot\boldsymbol{S})|\hat{S}(\hat{n})\rangle=|\hat{S}(\hat{n})\rangle$. The local states $|\Psi\rangle$ are chosen for FQ and AFQ phases as follows. (a) FQ1: $|\Psi\rangle=(|x\rangle+|y\rangle)/\sqrt{2}$; (b) AFQ1: $|\Psi_1\rangle=(|x\rangle+|y\rangle)/\sqrt{2}$ and $|\Psi_2\rangle=(|x\rangle-|y\rangle)/\sqrt{2}$; (c) FQ2: $|\Psi\rangle=(|x\rangle+|z\rangle)/\sqrt{2}$; (d) AFQ2: $|\Psi_1\rangle=(|x\rangle+|z\rangle)/\sqrt{2}$ and $|\Psi_2\rangle=(|x\rangle-|z\rangle)/\sqrt{2}$; (e) FQ3: $|\Psi\rangle=|z\rangle$; and (f) AFQ3: $|\Psi_1\rangle=(|x\rangle+|y\rangle)/\sqrt{2}$ and $|\Psi_2\rangle=|z\rangle$. Here the subscripts in $\Psi_{1,2}$ refer to sublattices 1 and 2.

B. Low-energy excitations

The low-energy excitations can be understood in the framework of the symmetry hierarchy as follows. (1) The spontaneous symmetry breaking is distinct in the different phases:

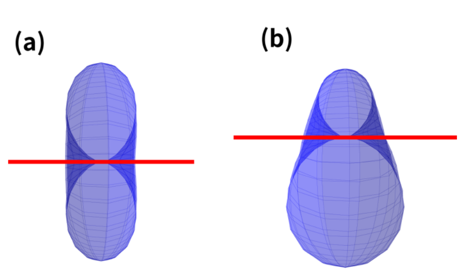

FIG. 2. Local spin density for (a) time-reversal invariant and (b) time-reversal breaking states. Red bars indicate the directions of $(|d_x|,|d_y|,|d_z|)$. Blue surfaces represent the spin density of a local wave function Ψ, which is defined as $|\langle\hat{S}(\hat{n})|\Psi\rangle|^2$. Here, $|\hat{S}(\hat{n})\rangle$ is the spin coherent state pointing along direction $\hat{n}$ and is defined by $(\hat{n}\cdot\boldsymbol{S})|\hat{S}(\hat{n})\rangle=|\hat{S}(\hat{n})\rangle$. The local states $|\Psi\rangle$ are chosen for (a) $|\Psi\rangle=(|x\rangle+|y\rangle)/\sqrt{2}$; (b) $|\Psi\rangle=(e^{i\pi/10}|x\rangle+|y\rangle)/\sqrt{2}$.

(a) SU(2) is broken in FQ1 (AFQ1), but $U(1)$ is not [i.e., $\mathrm{SU}(2)\times U(1)\to U(1)$]; (b) both SU(2) and $U(1)$ are broken in FQ2 (AFQ2) [i.e., $\mathrm{SU}(2)\times U(1)\to 1$]; and (c) neither SU(2) nor $U(1)$ is broken in FQ3 (AFQ3). (2) For FQ1, the ω_1^{FQ1} mode is gapless, while the other mode, ω_2^{FQ1}, is gapful. Since SU(2) is broken, the gapless Goldstone mode ω_1^{FQ1} tends to recover the symmetry. However, $U(1)$ is unbroken, so ω_2^{FQ1} is not required to be gapless as well. The gapless ω_1^{FQ1} mode corresponds to two-magnon excitations, while the gapful ω_2^{FQ1} mode corresponds to one-magnon excitations (see Appendix D). (3) For FQ2, there are two gapless Goldstone modes, ω_1^{FQ2} and ω_2^{FQ2}, because both SU(2) and $U(1)$ are broken. The ω_1^{FQ2} mode is an admixture of one- and two-magnon excitations, while the ω_2^{FQ2} mode consists of one-magnon excitations only. (4) For FQ3, there are two gapful modes, $\omega_1^{\mathrm{FQ3}}=\omega_2^{\mathrm{FQ3}}$, which are related to each other through the SU(2) symmetry. Both of them correspond to one-magnon excitations. (5) The AFQ1, AFQ2, and AFQ3 phases can be analyzed similarly.

The mean-field ground states and low-energy flavor-wave excitations for these six phases are summarized in Table II.

TABLE II. Summary of the $SU(2)_\gamma \times U(1) \times \mathcal{T} \times \mathcal{I}$-symmetric model defined in Eq. (9). The parameters ϑ and $\tilde{\vartheta}$ are given by $\sin^2\vartheta = \frac{2|K_2|+K_1+K_3}{4|K_2|+K_1+3K_3}$ and $\sin^2\tilde{\vartheta} = \frac{2K_2+K_1+K_3}{4K_2+K_1+3K_3}$, respectively. $\mathcal{R}(\chi,\theta,\phi,\varphi) = \mathrm{diag}(e^{i\frac{\phi}{2}\sigma^z}e^{i\frac{\theta}{2}\sigma^y}e^{i\frac{\chi}{2}\sigma^z}, e^{i\varphi})$ is an $SU(2)\times U(1)$ rotation. $A_K,\ B_K,\ C_K,\ D_K$, and $\gamma(\boldsymbol{k})$ are defined as follows: $A_K = \frac{2|K_2|-K_1+K_3-2K_1K_3/|K_2|}{4|K_2|+K_1+3K_3}$, $B_K = \frac{K_1+3K_3+2K_3(K_1+K_3)/|K_2|}{4|K_2|+K_1+3K_3}$, $C_K = (3+K_1/K_3)/2$, $D_K = 2K_2/K_3$, and $\gamma(\boldsymbol{k}) = Z^{-1}\sum_\delta e^{i\boldsymbol{k}\cdot\boldsymbol{\delta}}$, where $Z = 2D$ is the coordination number and $\boldsymbol{\delta}$ is a nearest-neighbor displacement. "1" refers to one-magnon excitations, "2" refers to two-magnon excitations, and "1+2" refers to an admixture of one- and two-magnon excitations.

	$\boldsymbol{d}$ vector(s)	Flavor-wave dispersion	Gap	Magnon
FQ1	$\boldsymbol{d} = \mathcal{R}(\chi,\theta,\phi,0)(1,0,0)^T$	$\omega_1^{\mathrm{FQ1}}(\boldsymbol{k}) = 2Z\|K_1\|[1-\gamma(\boldsymbol{k})]$	gapless	2
		$\omega_2^{\mathrm{FQ1}}(\boldsymbol{k}) = Z(\|K_1\|-K_3) + 2ZK_2\gamma(\boldsymbol{k})$	gapful	1
FQ2	$\boldsymbol{d} = \mathcal{R}(\chi,\theta,\phi,\varphi)(\cos\vartheta,0,\sin\vartheta)^T$	$\omega_1^{\mathrm{FQ2}}(\boldsymbol{k}) = 2Z\|K_2\|A_K(1-\gamma(\boldsymbol{k}))$	gapless	1 + 2
		$\omega_2^{\mathrm{FQ2}}(\boldsymbol{k}) = 2Z\|K_2\|\sqrt{[1-\gamma(\boldsymbol{k})][1+B_K\gamma(\boldsymbol{k})]}$		1
FQ3	$\boldsymbol{d} = \mathcal{R}(0,0,0,\varphi_i)(0,0,1)^T$	$\omega_1^{\mathrm{FQ3}}(\boldsymbol{k}) = \omega_2^{\mathrm{FQ3}}(\boldsymbol{k}) = 2Z[\|K_3\| + K_2\gamma(\boldsymbol{k})]$	gapful	1
AFQ1	$\boldsymbol{d}_1 = \mathcal{R}(\chi,\theta,\phi,0)(1,0,0)^T$	$\omega_1^{\mathrm{AFQ1}}(\boldsymbol{k}) = \omega_2^{\mathrm{AFQ1}}(\boldsymbol{k}) = 2ZK_1\sqrt{1-\gamma^2(\boldsymbol{k})}$	gapless	2
	$\boldsymbol{d}_2 = \mathcal{R}(\chi,\theta,\phi,0)(0,1,0)^T$	$\omega_3^{\mathrm{AFQ1}}(\boldsymbol{k}) = \omega_4^{\mathrm{AFQ1}}(\boldsymbol{k}) = Z(K_1-K_3)$	gapful	1
AFQ2	$\boldsymbol{d}_1 = \mathcal{R}(\chi,\theta,\phi,\varphi)(\cos\tilde{\vartheta},0,\sin\tilde{\vartheta})^T$	$\omega_1^{\mathrm{AFQ2}} = 2ZK_2A_K[1-\gamma(\boldsymbol{k})]$	gapless	1 + 2
	$\boldsymbol{d}_2 = \mathcal{R}(\chi,\theta,\phi,\varphi)(\cos\tilde{\vartheta},0,-\sin\tilde{\vartheta})^T$	$\omega_2^{\mathrm{AFQ2}} = 2ZK_2A_K[1+\gamma(\boldsymbol{k})]$		1 + 2
		$\omega_3^{\mathrm{AFQ2}} = 2ZK_2\sqrt{[1+\gamma(\boldsymbol{k})][1-B_K\gamma(\boldsymbol{k})]}$		1
		$\omega_4^{\mathrm{AFQ2}} = 2ZK_2\sqrt{[1-\gamma(\boldsymbol{k})][1+B_K\gamma(\boldsymbol{k})]}$		1
AFQ2	$\boldsymbol{d}_1 = \mathcal{R}(0,0,0,\varphi_i)(0,0,1)^T$	$\omega_1^{\mathrm{AFQ3}}(\boldsymbol{k}) = Z(K_3-K_1)$	gapful	2
	$\boldsymbol{d}_2 = \mathcal{R}(\chi_i,\theta_i,\phi_i,0)(1,0,0)^T$	$\omega_2^{\mathrm{AFQ3}}(\boldsymbol{k}) = 0 + O(\boldsymbol{k}^3)$	gapless	2
		$\omega_3^{\mathrm{AFQ3}}(\boldsymbol{k}) = Z\big[K_3\sqrt{C_K^2 - D_K^2\gamma^2(\boldsymbol{k})} + \frac{K_1-K_3}{2}\big]$	gapful	1
		$\omega_4^{\mathrm{AFQ3}}(\boldsymbol{k}) = Z\big[K_3\sqrt{C_K^2 - D_K^2\gamma^2(\boldsymbol{k})} + \frac{K_3-K_1}{2}\big]$	gapful	1

C. Spectral functions: a clue to the eightfold way

Inelastic neutron scattering measures the spin spectral function in $(\boldsymbol{q},\omega)$ space, which is defined as

$$S^{\alpha\beta}(\boldsymbol{q},\omega) = \mathrm{Im}\left\{ i\int_0^\infty dt\, e^{i\omega t}\langle[S^\alpha(\boldsymbol{q},t), S^\beta(-\boldsymbol{q},0)]\rangle \right\},$$

where we have set $\mu g_B = 1$ for simplicity. At zero temperature, $S^{\alpha\beta}(\boldsymbol{q},\omega)$ depends on the choice of the ground state. However, the spectral function

$$S(\boldsymbol{q},\omega) \equiv S^{xx}(\boldsymbol{q},\omega) + S^{yy}(\boldsymbol{q},\omega) + S^{zz}(\boldsymbol{q},\omega)$$

does not change qualitatively within a single phase. On the other hand, resonant inelastic x-ray scattering (RIXS) measures two-magnon processes, which is described by spin quadrupole spectral functions

$$Q^{\mu\nu}(\boldsymbol{q},\omega) = \mathrm{Im}\left\{ i\int_0^\infty dt\, e^{i\omega t}\langle[Q^\mu(\boldsymbol{q},t), Q^\nu(-\boldsymbol{q},0)]\rangle \right\},$$

and μ and ν denote $xy,\ yz,\ zx,\ x^2-y^2$, and $3z^2-r^2$. Similar to $S(\boldsymbol{q},\omega)$, the spin quadrupole spectral function,

$$Q(\boldsymbol{q},\omega) \equiv \sum_\mu Q^{\mu\mu}(\boldsymbol{q},\omega),$$

does not change qualitatively within a single phase as well. Therefore the spin spectral function $S(\boldsymbol{q},\omega)$ and the spin quadrupole spectral function $Q(\boldsymbol{q},\omega)$ can be used to detect flavor waves and distinguish the various FQ and AFQ phases.

In the flavor-wave mean-field theory, all the degenerate ground states can be obtained from one of them by an $SU(2)\times U(1)$ rotation of the $\boldsymbol{d}$ vector. We parametrize a general $SU(2)$ rotational matrix as

$$R = r_0\sigma^0 + i\sum_{n=1}^3 r_n\sigma^n, \tag{10}$$

where σ^0 are identity as well as $\sigma^1,\ \sigma^2$, and σ^3 are three Pauli matrices. Here, $\hat{r} = \{r_0, r_1, r_2, r_3\}$ is a four-dimensional real vector with $\sum_{n=0}^3 r^2 = 1$. Thus, apart from a global phase factor, two $\boldsymbol{d}$ vectors of two degenerate ground states, $\boldsymbol{d}$ and $\boldsymbol{d}'$, are related by a 3×3 matrix as follows:

$$\boldsymbol{d}' = \begin{pmatrix} e^{-i\phi}R & 0_{2,1} \\ 0_{1,2} & 1 \end{pmatrix}\boldsymbol{d}, \tag{11}$$

where $0_{1,2}(0_{2,1})$ is a $1\times 2(2\times 1)$ zero matrix. In the SU(3) Schwinger boson representation, the expression for the spin operators $\boldsymbol{S}$ depends on the parameters r_{0-3}.

Thus these spectral functions can be evaluated for each FQ or AFQ state; these functions are distinct in different phases but do not qualitatively change within a single phase. Moreover, $S(\boldsymbol{q},\omega)$ and $Q(\boldsymbol{q},\omega)$ *share the same structure* as long as the elementary excitations are flavor waves, as demonstrated in Fig. 4. Namely, $Q(\boldsymbol{q},\omega)$ has the same dispersion as $S(\boldsymbol{q},\omega)$, and difference between them is in the spectral weight. *This similarity provides evidence for the underlying* SU(3) *structure and serves as a clue to the eightfold way.* The details of these spectral functions for all FQ and AFQ phases can be found in see Appendix E.

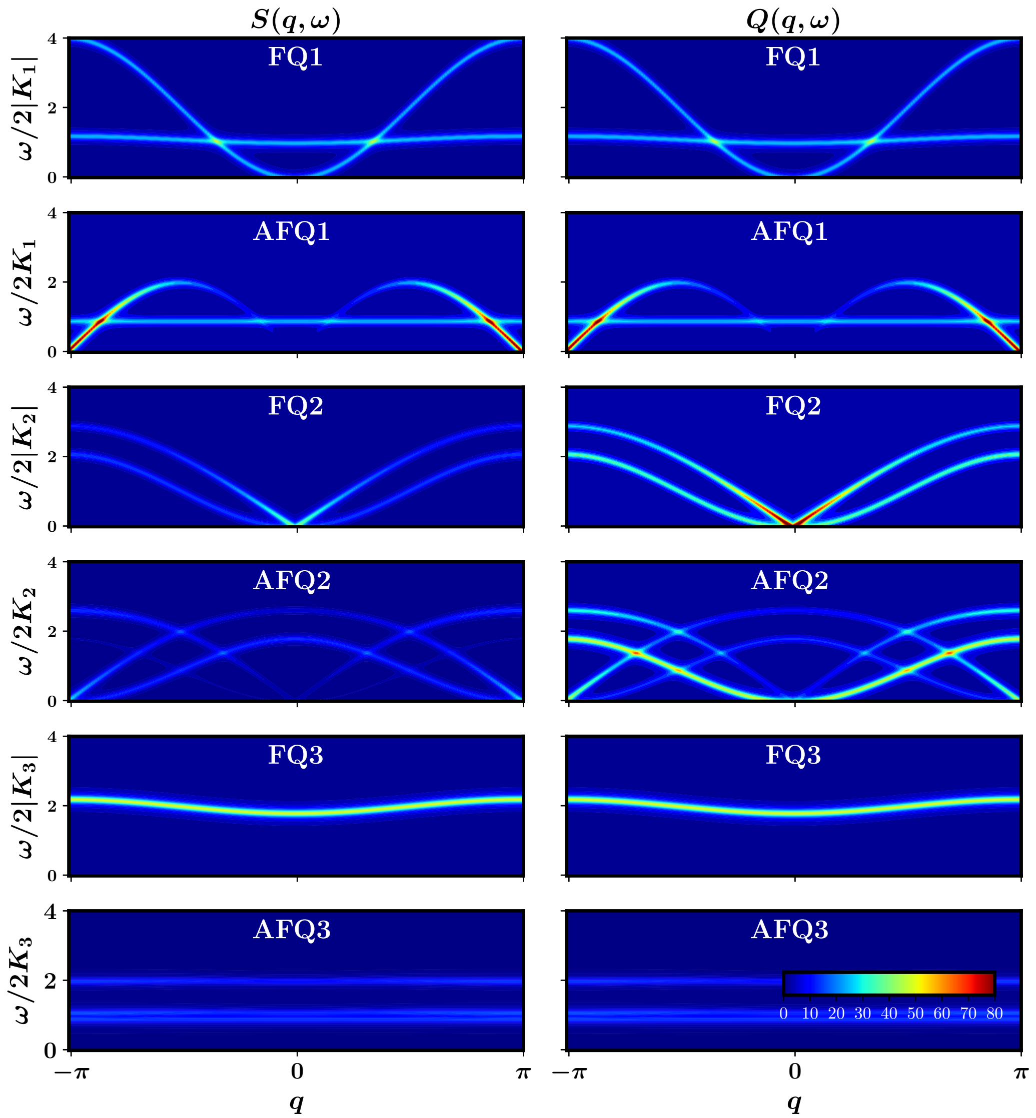

FIG. 4. The spin spectral functions $S(\boldsymbol{q},\omega)$ and the spin quadrupole spectral functions $Q(\boldsymbol{q},\omega)$ for the FQ and AFQ phases. Here, we set $K_2 = K_3 = 0.1K_1$ for FQ1 and AFQ1, $K_1 = K_3 = 0.1K_2$ for FQ2 and AFQ2, and $K_1 = K_2 = 0.1K_3$ for FQ3 and AFQ3.

IV. BEYOND THE MEAN-FIELD THEORY

A. Effective Hamiltonian in the AFQ3 phase: a possible emergent $S = 1/2$ gapless spin liquid

In the mean-field solution, the AFQ3 ground states are locally degenerate inside a bulk energy gap. This huge degeneracy arises from the unperturbative Hamiltonian $K_3\mathcal{H}_3$, of which ground state subspace is spanned by the local basis $\{|x\rangle_i, |y\rangle_i\}$ on sublattice-2 and $\{|z\rangle_i\}$ on sublattice-1, as shown in Fig. 5(a). And the degeneracy is expected to be lifted by a small but finite K_1 and K_2. To address this case and go beyond the mean-field theory, we consider perturbations of up to the third order in the limit $K_3 \gg |K_{1(2)}|$, where the unperturbative energy gap is about ZK_3. What we need is to include all the possible perturbations of $\mathcal{H}_1$ and $\mathcal{H}_2$ and project the states into the subspace of unperturbative ground states by a projector $\mathcal{P}$.

We begin with two-site Hamitonians h_i, $i = 1, 2, 3$, which is the simplest case of the Hamiltonians $\mathcal{H}_i$ defined in Eq. (8), and consider their matrix elements. Firstly, $h_3 = Q_1^{3z^2-r^2}Q_2^{3z^2-r^2}$, which is diagonal in the basis $\{|\sigma_1\sigma_2\rangle\}$, where $\sigma_{1,2} = x, y, z$. Secondly, $h_1 = S_1^zS_2^z + Q_1^{xy}Q_2^{xy} + Q_1^{x^2-y^2}Q_2^{x^2-y^2}$, and we have

$$h_1|\sigma_1\sigma_2\rangle = \begin{cases} |\sigma_1\sigma_2\rangle, & \sigma_1 = \sigma_2 \neq z, \\ 2|\sigma_2\sigma_1\rangle, & \sigma_1 = x(y), \sigma_2 = y(x), \\ 0, & \text{otherwise}. \end{cases} \tag{12}$$

Thirdly, $h_2 = S_1^xS_2^x + S_1^yS_2^y + Q_1^{yz}Q_2^{yz} + Q_1^{zx}Q_2^{zx}$, we have

$$h_2|\sigma_1\sigma_2\rangle = \begin{cases} 2|\sigma_2\sigma_1\rangle, & \sigma_1 = x, y(z) \text{ and } \sigma_2 = z(x, y), \\ 0, & \text{otherwise}. \end{cases} \tag{13}$$

Taking into account all the nonzero matrix elements, the leading perturbation is of the third order and the effective Hamiltonian reads

$$\mathcal{H}_{\text{eff}} = \frac{K_1K_2^2}{K_3^2}\mathcal{P}\mathcal{H}_2\mathcal{H}_1\mathcal{H}_2\mathcal{P}. \tag{14}$$

Regarding the projector $\mathcal{P}$, $\mathcal{H}_{\rm eff}$ can be written as a $\mathcal{H}_1$ type Hamiltonian defined on one of the sublattices.

As an example, consider a square lattice; the spins have a quadrupolar order on one of the two sublattices, and we have the following effective Hamiltonian on the other sublattice:

$$\mathcal{H}_{\rm eff} = \tilde{J}_1 \sum_{\langle ij\rangle_1} \mathcal{P}\big(S_i^z S_j^z + Q_i^{xy} Q_j^{xy} + Q_i^{x^2-y^2} Q_j^{x^2-y^2}\big)\mathcal{P} + \tilde{J}_2 \sum_{\langle ij\rangle_2} \mathcal{P}\big(S_i^z S_j^z + Q_i^{xy} Q_j^{xy} + Q_i^{x^2-y^2} Q_j^{x^2-y^2}\big)\mathcal{P},$$

where $\langle ij\rangle_{1(2)}$ denotes a pair of (next) nearest neighboring sites on the sublattice, $\tilde{J}_1 = 2K_1K_2^2/K_3^2$ and $\tilde{J}_2 = K_1K_2^2/K_3^2$. Note that the relation $\tilde{J}_2/\tilde{J}_1 = 1/2$ is guaranteed by the fact that there are two paths contribute to $\tilde{J}_1$ while only one path contributes to $\tilde{J}_2$, as illustrated in Fig. 5

Thus there emerges an effective spin-1/2 $\tilde{J}_1$-$\tilde{J}_2$ Heisenberg model constructed by the $\mathrm{SU}(2)_\gamma$ generators. When $K_1 < 0$, $\tilde{J}_{1(2)} < 0$, and the ground state is of ferromagnetic order. When $K_1 > 0$, $\tilde{J}_1 = 2\tilde{J}_2 > 0$, a gapless quantum spin liquid (QSL) ground state [26] may be favored, as suggested by variational Monte Carlo [27–29] and density matrix renormalization group (DMRG) [30]. It is worth noting that the ground states of spin-1/2 J_1-J_2 Heisenberg model still remains a controversial issue, and various numerical approaches lead to several contradictory results. Other possible ground states include Néel order [31,32] (by PEPS), gapful spin liquid [33] (by DMRG), and plaquette valence-bond solid [34–37] (by exact diagonalization, tensor network, and DMRG). Despite of the controversy, we would like to propose that a QSL state with effective spin $S = 1/2$ (or other ordered states) may coexist with gapful quadrupolar order in a quantum spin-1 system.

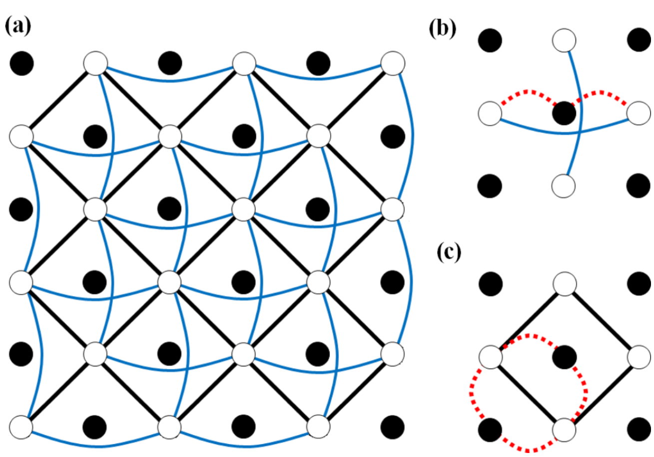

FIG. 5. Solid circles form sublattice-1 where all the spins are in the $|z\rangle$ state and open circles form sublattice 2 where all the spins are in $|x\rangle$ or $|y\rangle$ state. (a) Emergent $\tilde{J}_1 - \tilde{J}_2$ super square lattice with black solid lines for $\tilde{J}_1$ bonds and blue curve lines for $\tilde{J}_2$ bonds. (b) One path to achieve J_2 bond. (c) Two paths to achieve $\tilde{J}_1$ bonds. (b) and (c) indicate that $\tilde{J}_2/\tilde{J}_1 = 0.5$.

B. Hydrodynamics modes in a quantum spin-orbital liquid: in analogy to QCD

Now we consider a quantum spin-orbital liquid ground state in the $\mathrm{SU}(2)\times U(1)$ symmetric model, where neither SU(2) nor $U(1)$ symmetry is broken and all the correlation functions of the operators $\{\boldsymbol{S},\boldsymbol{Q}\}$ are short ranged. If there does exist such a spin-orbital liquid state, the low-energy excitations can be described by the fields of $\{\boldsymbol{S},\boldsymbol{Q}\}$ and can be classified according to the $\mathrm{SU}(2)\times U(1)$ symmetry. Because of the short-range correlation, these excitations are gapful. In analogy to QCD, we will demonstrate below that these excitation gaps must satisfy some relations due to the symmetry hierarchy $\mathrm{SU}(3) \supset \mathrm{SU}(2)\times U(1)$.

An interesting observation is that the three local spin states $|x\rangle, |y\rangle, |z\rangle$ can be naturally in analogy with the u, d, s quarks in particle physics in the fundamental representation of SU(3) symmetry as follows:

$$\begin{aligned} |x\rangle &\longleftrightarrow u,\\ |y\rangle &\longleftrightarrow d,\\ |z\rangle &\longleftrightarrow s. \end{aligned} \tag{15}$$

The quark model is a successful theory of the strong interaction, which is known as QCD. According to Gell-Mann's argument: (1) there exists an additive quantum number called strangeness is conserved in addition to isospin SU(2) symmetry; (2) in very strong interactions region, the symmetry is SU(3) rather then the $\mathrm{SU}(2)\times U(1)$; and (3) in medium strong interactions region, the SU(3) breaks into $\mathrm{SU}(2)\times U(1)$, i.e., isospin SU(2) and hypercharge $U(1)$. This symmetry hierarchy is exactly as the same as what we discuss in our spin-1 systems. Moreover, the SU(3) octet $\{\boldsymbol{S},\boldsymbol{Q}\}$ can be mapped to high-energy particles, e.g., the light spin-0 mesons, in addition to the SU(3) triplet mapping in Eq. (15) as follows:

$$\begin{aligned}
\tfrac{1}{2}(iS^x - Q^{yz}) &\longleftrightarrow K^0 \quad (d\bar{s}),\\
\tfrac{1}{2}(-iS^y - Q^{zx}) &\longleftrightarrow K^+ \quad (u\bar{s}),\\
\tfrac{1}{2}(iS^x + Q^{yz}) &\longleftrightarrow \bar{K}^0 \quad (s\bar{d}),\\
\tfrac{1}{2}(-iS^y + Q^{zx}) &\longleftrightarrow K^- \quad (s\bar{u}),\\
\tfrac{1}{2}(iS^z - Q^{xy}) &\longleftrightarrow \pi^+ \quad (u\bar{d}),\\
\tfrac{1}{2}(-iS^z - Q^{xy}) &\longleftrightarrow \pi^- \quad (d\bar{u}),\\
Q^{x^2-y^2} &\longleftrightarrow \pi^0 \quad (u\bar{u}, d\bar{d}),\\
Q^{3z^2-r^2} &\longleftrightarrow \eta \quad (u\bar{u}, d\bar{d}, s\bar{s}).
\end{aligned} \tag{16}$$

For the shorthand, let us define the following operators:

$$\begin{aligned}
K^0 &= (iS^x - Q^{yz})/2,\\
K^+ &= (-iS^y - Q^{zx}),\\
\bar{K}^0 &= (-iS^x - Q^{yz})/2,\\
K^- &= (iS^y - Q^{zx})/2,\\
\pi^+ &= (iS^z - Q^{xy})/2,\\
\pi^- &= (-iS^z - Q^{xy})/2,\\
\pi^0 &= Q^{x^2-y^2},\\
\eta &= Q^{3z^2-r^2}.
\end{aligned} \tag{17}$$

Thus, in the hydrodynamic limit, $\boldsymbol{q} \to 0$ and $\omega \to 0$, the collective modes in a quantum spin-orbital liquid can be described by the fields of K^0, $\bar{K}^0$, $K^{\pm}$, π^0, $\pi^{\pm}$, and η. And we expect that each hydrodynamic mode has an excitation gap M. The excitaiton gap is nothing but the mass of the corresponding particle. By the $\mathrm{SU}(2) \times U(1)$ symmetry, we deduce that these gaps must satisfy the relations,

$$M_{K^0} = M_{K^+}, \tag{18a}$$

$$M_{\bar{K}^0} = M_{K^-}, \tag{18b}$$

$$M_{\pi^{\pm}} = M_{\pi^0} = M_{\pi}, \tag{18c}$$

as well as the famous Gell-Mann-Okubo formula [38]

$$2(M_{K^+} + M_{K^-}) = 3M_{\eta} + M_{\pi}. \tag{18d}$$

V. SUMMARY

In summary, we have revealed hidden SU(2) symmetries in spin-1 quantum magnets, studied them in accordance with the $\mathrm{SU}(3) \supset \mathrm{SU}(2) \times U(1)$ symmetry hierarchy, demonstrated novel emergent phenomena, and found some clues to the emergent eightfold way. These SU(2) symmetries may be realized in cold atoms as well as d^8 and/or d^6 electrons with the proper specific choices of the spin-orbital couplings.

ACKNOWLEDGMENTS

This work is supported in part by National Key Research and Development Program of China (No. 2016YFA0300202), National Natural Science Foundation of China (No. 11774306), and the Strategic Priority Research Program of Chinese Academy of Sciences (No. XDB28000000). J.J.M. is supported by China Postdoctoral Science Foundation (Grant No. 2017M620880) and the National Natural Science Foundation of China (Grant No. 1184700424).

APPENDIX A: FUNDAMENTALS OF SU(3) LIE ALGEBRA

The eight Gell-Mann matrices are defined as

$$\lambda_1 = \begin{pmatrix} 0 & 1 & 0 \\ 1 & 0 & 0 \\ 0 & 0 & 0 \end{pmatrix}, \quad \lambda_2 = \begin{pmatrix} 0 & -i & 0 \\ i & 0 & 0 \\ 0 & 0 & 0 \end{pmatrix},$$
$$\lambda_3 = \begin{pmatrix} 1 & 0 & 0 \\ 0 & -1 & 0 \\ 0 & 0 & 0 \end{pmatrix}, \quad \lambda_4 = \begin{pmatrix} 0 & 0 & 1 \\ 0 & 0 & 0 \\ 1 & 0 & 0 \end{pmatrix}, \tag{A1}$$
$$\lambda_5 = \begin{pmatrix} 0 & 0 & -i \\ 0 & 0 & 0 \\ i & 0 & 0 \end{pmatrix}, \quad \lambda_6 = \begin{pmatrix} 0 & 0 & 0 \\ 0 & 0 & 1 \\ 0 & 1 & 0 \end{pmatrix},$$
$$\lambda_7 = \begin{pmatrix} 0 & 0 & 0 \\ 0 & 0 & -i \\ 0 & i & 0 \end{pmatrix}, \quad \lambda_8 = \frac{1}{\sqrt{3}}\begin{pmatrix} 1 & 0 & 0 \\ 0 & 1 & 0 \\ 0 & 0 & -2 \end{pmatrix}.$$

The generators of SU(3) Lie group are given by $T_i = \lambda_i/2,\ i = 1, \ldots, 8$.

In SU(3) representations, a state in an irreducible representation (IR) is labeled by (p, q), corresponding to the weight vector $\boldsymbol{\mu} = p\boldsymbol{\mu}^1 + q\boldsymbol{\mu}^2$, where $\boldsymbol{\mu}^1 = (1/2, \sqrt{3}/6)$ and

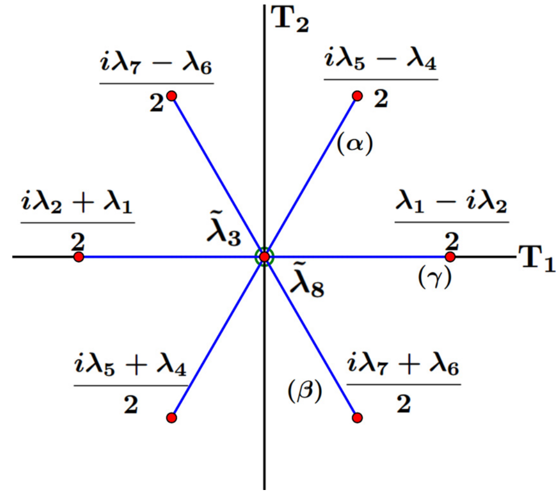

FIG. 6. Roots of SU(3) Lie algebra. There are two simple roots, $\boldsymbol{\alpha} = (\frac{1}{2}, \frac{\sqrt{3}}{2})$ and $\boldsymbol{\beta} = (\frac{1}{2}, -\frac{\sqrt{3}}{2})$. $\boldsymbol{\gamma} = \boldsymbol{\alpha} + \boldsymbol{\beta} = (1, 0)$ is the other positive root. $\{\frac{iT_2+T_1}{2}, \frac{T_1-iT_2}{2}, T_3\}$ are three generators of the subalgebra $\mathrm{SU}(2)_{\gamma}$, and so on and so forth.

$\boldsymbol{\mu}^2 = (1/2, -\sqrt{3}/6)$. The weights are defined by the eigenvalues of the Cartan generators H_1 and H_2, $H_i|\boldsymbol{\mu}\rangle = \mu_i|\boldsymbol{\mu}\rangle$, where $i = 1$ and 2. So that $T_3|(p, q)\rangle = (p+q)/2|(p, q)\rangle$ and $T_8|(p, q)\rangle = \sqrt{3}(p-q)/6|(p, q)\rangle$. An IR is characterized by the highest weight (n, m). Thus a state in a SU(3) IR can be written as $|(n, m), (p, q)_k\rangle$. Note that there may exist more than one (p, q) state in IR (n, m), these different (p, q) states are distinguished by the subscript k, which will be neglected when there is only one (p, q) state.

APPENDIX B: SU(3) STRUCTURE AND HIDDEN SU(2) SYMMETRIES

Firstly, it is straightforward to examine the SU(3) Lie algebra relation among $\{\boldsymbol{S}, \boldsymbol{Q}\}$ through the commutators $[S^{\alpha}, S^{\beta}]$, $[S^{\alpha}, Q^{\mu}]$, and $[Q^{\mu}, Q^{\nu}]$ directly. As mentioned, besides the SO(3) subalgebra of $\{S^x, S^y, S^z\}$, there are other SU(2) subalgebras belonging to the SU(3) Lie algebra.

In order to find out the other SU(2) subalgebras, we consider the Cartan subalgebra H, the largest commutative subalgebra, of the SU(3) Lie algebra, which can be chosen to be made of linear combinations of two commutative operators $H_1 = T_3$ and $H_2 = T_8$, where $T_i = \lambda_i/2$ and satisfy $\mathrm{Tr}(H_i H_j) = \frac{1}{2}\delta_{ij}$. An SU(2) subalgebra can be constructed as follows. Let us select an operator in the Cartan subalgebra H, which serves as J^z in the SU(2) algebra. Writing $\boldsymbol{H} = \{H_1, H_2\}$, we have $J^z = |\boldsymbol{\alpha}|^{-2}\boldsymbol{\alpha} \cdot \boldsymbol{H}$, where $\boldsymbol{\alpha}$ is a two-dimensional vector. Then the raising and lowering operators $J^{\pm}$ can be obtained through $J^{\pm} = |\boldsymbol{\alpha}|^{-1}E_{\pm\boldsymbol{\alpha}}$, with $\boldsymbol{\alpha}$ a root vector. It is easy to verify that $[J^z, J^{\pm}] = \pm J^{\pm}$ and $[J^+, J^-] = 2J_z$. So that a nonzero root $\boldsymbol{\alpha}$ of SU(3) will give rise to an SU(2) subgroup.

The roots of SU(3) algebra are nothing but the weights of its adjoint representation (1,1), which are plotted in Fig. 6. It is clear that there are three pairs of nonzero roots, $\{\pm\boldsymbol{\alpha}, \pm\boldsymbol{\beta}, \pm\boldsymbol{\gamma}\}$, where $\boldsymbol{\alpha} = (\frac{1}{2}, \frac{\sqrt{3}}{2})$ and $\boldsymbol{\beta} = (\frac{1}{2}, -\frac{\sqrt{3}}{2})$ are two simple roots, and $\boldsymbol{\gamma} = (1, 0)$ is the other positive root with

$\boldsymbol{\gamma} = \boldsymbol{\alpha} + \boldsymbol{\beta}$. So that $\boldsymbol{\alpha}, \boldsymbol{\beta}, \boldsymbol{\gamma}$ give rise to three SU(2) subalgebras, whose generators are given as follows: $\mathrm{SU}(2)_\alpha : \{T_4, T_5, \boldsymbol{\alpha}\cdot\boldsymbol{H}\}$, $\mathrm{SU}(2)_\beta : \{T_6, T_7, \boldsymbol{\beta}\cdot\boldsymbol{H}\}$ and $\mathrm{SU}(2)_\gamma : \{T_1, T_2, \boldsymbol{\gamma}\cdot\boldsymbol{H}\}$. In terms of $\boldsymbol{S}$ and $\boldsymbol{Q}$, the generators of the three SU(2) subgroups read

$$\begin{aligned} &\mathrm{SU}(2)_\alpha : \left\{Q^{zx}, S^y, \frac{1}{2}Q^{x^2-y^2} + \frac{\sqrt{3}}{2}Q^{3z^2-r^2}\right\}, \\ &\mathrm{SU}(2)_\beta : \left\{Q^{yz}, S^x, \frac{1}{2}Q^{x^2-y^2} - \frac{\sqrt{3}}{2}Q^{3z^2-r^2}\right\}, \\ &\mathrm{SU}(2)_\gamma : \left\{Q^{xy}, S^z, Q^{x^2-y^2}\right\}. \end{aligned} \tag{B1}$$

The underlying SU(3) structure and the hidden SU(2) symmetries will be more transparent in the Cartesian coordinate representation of spin states,

$$|x\rangle = i\frac{|1\rangle - |-1\rangle}{\sqrt{2}},\ |y\rangle = \frac{|1\rangle + |-1\rangle}{\sqrt{2}},\ |z\rangle = -i|0\rangle. \tag{B2}$$

It is easy to verify that $|\alpha\rangle$ is time-reversal invariant and satisfy the relations $\langle\alpha|\beta\rangle = \delta_{\alpha\beta}$ and $S^\alpha|\beta\rangle = i\epsilon^{\alpha\beta\gamma}|\gamma\rangle$, where $\alpha, \beta, \gamma = x, y, z$ and $\epsilon^{\alpha\beta\gamma}$ is the three-rank antisymmetric tensor. Thus a spin state can be expressed as follows:

$$|\boldsymbol{d}\rangle = d^x|x\rangle + d^y|y\rangle + d^z|z\rangle, \tag{B3}$$

where $\boldsymbol{d} = (d^x, d^y, d^z)$ is a complex vector, and normalization condition is given by $|\boldsymbol{d}|^2 = 1$. So that a time-reversal invariant state is given by a real vector $\boldsymbol{d}$ up to a global phase factor and characterized by $\langle\boldsymbol{d}|\boldsymbol{S}|\boldsymbol{d}\rangle = 0$. The expectation values for $\{\boldsymbol{S}, \boldsymbol{Q}\}$ can be expressed in terms of the $\boldsymbol{d}$ vector, $\langle S^\alpha\rangle = -i\epsilon_{\alpha\beta\gamma}\bar{d}^\beta d^\gamma$, $\langle Q^{\alpha\beta}\rangle|_{\alpha\neq\beta} = -(\bar{d}^\alpha d^\beta + \bar{d}^\beta d^\alpha)$, $\langle Q^{x^2-y^2}\rangle = |d^y|^2 - |d^x|^2$ and $\langle Q^{3z^2-r^2}\rangle = \frac{1}{\sqrt{3}}(2|d^z|^2 - |d^y|^2 - |d^x|^2)$, where $\bar{d}^\alpha$ is the conjugate complex number of d^α. Then the path integral for a spin $S = 1$ system can be written as in Eq. (7), where the Hamiltonian $\mathcal{H}$ is given by Eq. (2), while the operators $\boldsymbol{S}$ and $\boldsymbol{Q}$ are replaced by their expectation values as follows:

$$\begin{pmatrix} S^x \\ S^y \\ S^z \\ Q^{x^2-y^2} \\ Q^{3z^2-r^2} \\ Q^{xy} \\ Q^{yz} \\ Q^{zx} \end{pmatrix} = \begin{pmatrix} +\boldsymbol{d}^\dagger\lambda_7\boldsymbol{d} \\ -\boldsymbol{d}^\dagger\lambda_5\boldsymbol{d} \\ +\boldsymbol{d}^\dagger\lambda_2\boldsymbol{d} \\ -\boldsymbol{d}^\dagger\lambda_3\boldsymbol{d} \\ -\boldsymbol{d}^\dagger\lambda_8\boldsymbol{d} \\ -\boldsymbol{d}^\dagger\lambda_1\boldsymbol{d} \\ -\boldsymbol{d}^\dagger\lambda_6\boldsymbol{d} \\ -\boldsymbol{d}^\dagger\lambda_4\boldsymbol{d} \end{pmatrix}. \tag{B4}$$

Now it is clear that the unitary transformation of the three dimensional complex $\boldsymbol{d}$ vector (apart from a global phase factor) gives rise to the underlying SU(3) structure. Thus the SU(3) algebra of $\{\boldsymbol{S}, \boldsymbol{Q}\}$ can be visualized from Eq. (B4). Since the complex $\boldsymbol{d}$ vector transfer as a 1-rank tensor under the SU(3) rotations, one can find how $\boldsymbol{S}$ and $\boldsymbol{Q}$ and other physical quantities will transfer under SU(3) as well, which can be written in bilinear or biquadratic terms of $\boldsymbol{d}$ and $\bar{\boldsymbol{d}}$ in the path integral.

APPENDIX C: $\mathrm{SU}(2)_\gamma$ SYMMETRIC STATES/HAMILTONIANS

In the language of group theory, the three components of $\boldsymbol{d}$ belong to the three-dimensional (3D) fundamental representation $3 \equiv (1, 0)$ of SU(3) group, and those of $\bar{\boldsymbol{d}}$ belong to its complex conjugate representation $\bar{3} \equiv (0, 1)$. So that each $(\bar{\boldsymbol{d}}, \boldsymbol{d})$ bilinear term belongs to the representations $\bar{3} \otimes 3 = 1 \oplus 8$, where $1 \equiv (0, 0)$ and $8 \equiv (1, 1)$. Explicitly, $|\boldsymbol{d}|^2$ belongs to the 1D IR (0,0), and $(\boldsymbol{S}, \boldsymbol{Q})$ belong to the 8D IR (3,3). Furthermore, each $(\boldsymbol{S}, \boldsymbol{Q})$ bilinear term in Eq. (2) belongs to the representations $(1, 1) \otimes (1, 1) = (0, 0) \oplus (1, 1) \oplus (1, 1) \oplus (3, 0) \oplus (0, 3) \oplus (2, 2)$. Therefore we are able to classify the terms in Eq. (2) according to group theory and find possible spin Hamiltonians respecting the hidden SU(2) symmetries.

Begin with $\boldsymbol{d}$ vector and its complex conjugate $\bar{\boldsymbol{d}}$, the Cartesian coordinate representation of the three spin-1 states is isomorphic to SU(3) IR (1,0),

$$\begin{aligned} &|(1,0),(1,0)\rangle \longleftrightarrow |x\rangle \longleftrightarrow d^x, \\ &|(1,0),(-1,1)\rangle \longleftrightarrow |z\rangle \longleftrightarrow d^z, \\ &|(1,0),(0,-1)\rangle \longleftrightarrow |y\rangle \longleftrightarrow d^y, \end{aligned} \tag{C1}$$

and its complex conjugate representation (0,1),

$$\begin{aligned} &|(0,1),(0,1)\rangle \longleftrightarrow \langle y| \longleftrightarrow \bar{d}^y, \\ &|(0,1),(1,-1)\rangle \longleftrightarrow -\langle z| \longrightarrow -\bar{d}^z, \\ &|(0,1),(-1,0)\rangle \longleftrightarrow \langle x| \longleftrightarrow \bar{d}^x, \end{aligned} \tag{C2}$$

where $|(m, n), (p, q)\rangle$ was defined in previous section. Then $(\boldsymbol{S}, \boldsymbol{Q})$ can be obtained through $(0, 1) \otimes (1, 0) = (0, 0) \oplus (1, 1)$, which belong to the 8D IR (1,1),

$$\begin{aligned} &|(1,1),(1,1)\rangle \longleftrightarrow -\tfrac{iS^z+Q^{xy}}{2}, \\ &|(1,1),(-1,2)\rangle \longleftrightarrow \tfrac{iS^x-Q^{yz}}{2}, \\ &|(1,1),(2,-1)\rangle \longleftrightarrow -\tfrac{iS^y-Q^{zx}}{2}, \\ &|(1,1),(0,0)_1\rangle \longleftrightarrow \tfrac{-\sqrt{6}Q^{3z^2-r^2}-\sqrt{2}Q^{x^2-y^2}}{4}, \\ &|(1,1),(0,0)_2\rangle \longleftrightarrow \tfrac{-\sqrt{2}Q^{3z^2-r^2}+\sqrt{6}Q^{x^2-y^2}}{4}, \\ &|(1,1),(1,-2)\rangle \longleftrightarrow \tfrac{iS^x+Q^{yz}}{2}, \\ &|(1,1),(-2,1)\rangle \longleftrightarrow -\tfrac{iS^y+Q^{zx}}{2}, \\ &|(1,1),(-1,-1)\rangle \longleftrightarrow \tfrac{iS^z-Q^{xy}}{2}. \end{aligned} \tag{C3}$$

In what follows, we shall construct $\mathrm{SU}(2)_{\boldsymbol{\gamma}}$ symmetric two-body interactions in terms of bilinear forms of $(\boldsymbol{S}, \boldsymbol{Q})$. As mentioned, such bilinear forms belong to the representations $(1, 1) \otimes (1, 1) = (0, 0) \oplus (1, 1) \oplus (1, 1) \oplus (3, 0) \oplus (0, 3) \oplus (2, 2)$. Firstly we shall find out all the $\mathrm{SU}(2)_{\boldsymbol{\gamma}}$ symmetric states in the IR decomposition of $(1, 1) \otimes (1, 1)$, which would be annihilated by both the raising operator E_γ and the lowering operator $E_{-\gamma}$. According to the block diagram shown in Fig. 7, there exist six linear independent states in the IR decomposition. We list six linear independent

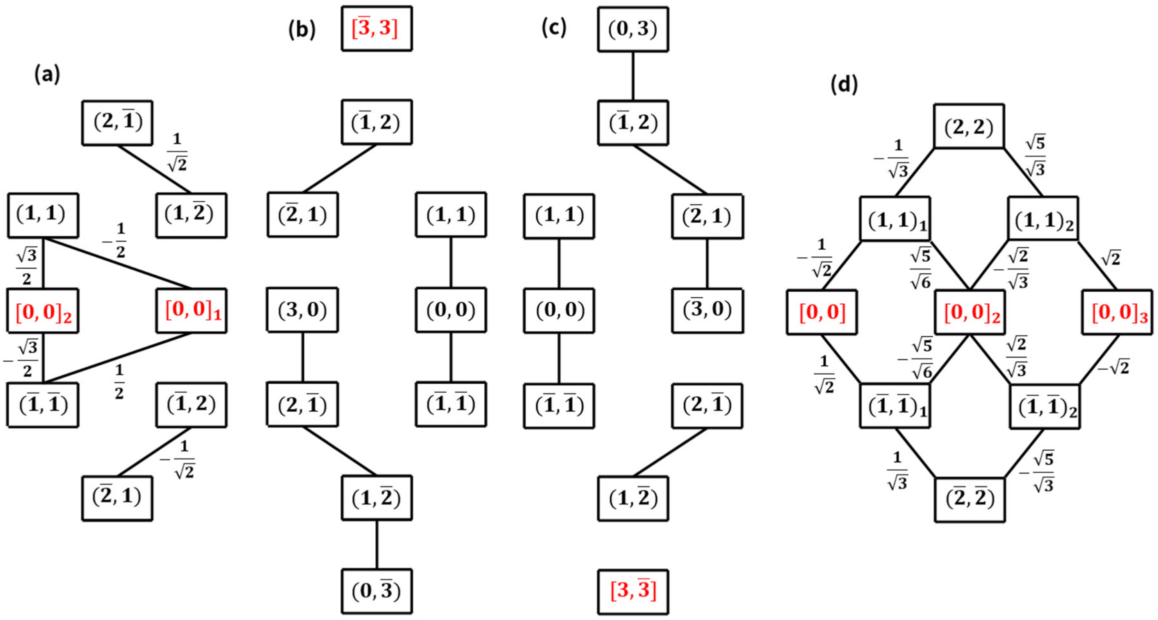

FIG. 7. The block diagrams are graphical notation of representations (1,1), (3,0), (0,3), and (2,2). The black solid lines between two block denotes the raising operator E_γ (upward) or lowering operator $E_{-\gamma}$ (downward). The states marked in red can be utilized to construct $SU(2)_\gamma$ symmetric states which will be annihilated by E_γ and $E_{-\gamma}$.

self-conjugate $SU(2)_{\boldsymbol{\gamma}}$ symmetric states as follows:

$$\begin{aligned}
\Gamma_0 &= |(0,0),(0,0)\rangle,\\
\Gamma_1 &= |(1,1),(0,0)_2\rangle_S+\sqrt{3}|(1,1),(0,0)_1\rangle_S,\\
\Gamma_2 &= |(1,1),(0,0)_2\rangle_A+\sqrt{3}|(1,1),(0,0)_1\rangle_A,\\
\Gamma_3 &= |(3,0),(-3,3)\rangle+|(0,3),(3,-3)\rangle,\\
\Gamma_4 &= i|(3,0),(-3,3)\rangle-i|(0,3),(3,-3)\rangle,\\
\Gamma_5 &= \sqrt{3}|(2,2),(0,0)_2\rangle-|(2,2),(0,0)_3\rangle\\
&\quad-\sqrt{5}|(2,2),(0,0)_1\rangle.
\end{aligned} \tag{C4}$$

Note that we have already made the bilinear forms symmetrized or antisymmetrized, where $|(1,1),(0,0)_2\rangle_S$ is a symmetrized state and $|(1,1),(0,0)_2\rangle_A$ is an antisymmetric state. All the possible $SU(2)_{\boldsymbol{\gamma}}$ symmetric states can be written as a linear combination of $\Gamma_n, n=0,\dots,5$ in Eq. (C4). Expanding Γ_n in terms of $(1,1)\otimes(1,1)$ states, $|(1,1),(p_1,q_1)\rangle\otimes|(1,1),(p_2,q_2)\rangle$, through SU(3) Clebsch-Gordan coefficients, and replacing abstract states $|(1,1),(p,q)\rangle$ by physical operators $(\boldsymbol{S},\boldsymbol{Q})$, eventually we obtain all the $SU(2)_\gamma$ symmetric spin Hamiltonians.

With the help of SU(3) Clebsch-Gordan coefficients, the $SU(2)_\gamma$ symmetric states in Eq. (C4) can be re-expressed in terms of states in IR (1,1) as follows:

$$\begin{aligned}
\Gamma_0 &= \frac{1}{\sqrt{8}}(|[0,0]_1\rangle_i|[0,0]_1\rangle_j+|[0,0]_2\rangle_i|[0,0]_2\rangle_j)\\
&\quad+\frac{1}{\sqrt{8}}(|[1,1]\rangle_i|[-1,-1]\rangle_j-|[-1,2]_2\rangle_i|[1,-2]_2\rangle_j-|[2,-1]_2\rangle_i|[-2,1]_2\rangle_j+(i\leftrightarrow j)),\\
\Gamma_1 &= \frac{1}{\sqrt{20}}(2|[2,-1]\rangle_i|[-2,1]\rangle_j+2|[-1,2]\rangle_i|[1,-2]\rangle_j+4|[1,1]\rangle_i|[-1,-1]\rangle_j+(i\leftrightarrow j))\\
&\quad+\frac{1}{\sqrt{20}}(-2|[0,0]_1\rangle_i|[0,0]_1\rangle_j+2|[0,0]_2\rangle_i|[0,0]_2\rangle_j-2\sqrt{3}|[0,0]_1\rangle_i|[0,0]_2\rangle_j-2\sqrt{3}|[0,0]_2\rangle_i|[0,0]_1\rangle_j),\\
\Gamma_2 &= (|[2,-1]\rangle_i|[-2,1]\rangle_j-|[-1,2]\rangle_i|[1,-2]\rangle_j-(i\leftrightarrow j)),\\
\Gamma_3 &= \frac{1}{\sqrt{2}}(|[-1,2]\rangle_i|[-2,1]\rangle_j+|[1,-2]\rangle_i|[2,-1]\rangle_j-(i\leftrightarrow j)),\\
\Gamma_4 &= \frac{i}{\sqrt{2}}(|[-1,2]\rangle_i|[-2,1]\rangle_j-|[1,-2]\rangle_i|[2,-1]\rangle_j-(i\leftrightarrow j)),\\
\Gamma_5 &= \frac{1}{\sqrt{40}}(3|[2,-1]\rangle_i|[-2,1]\rangle_j+3|[-1,2]\rangle_i|[1,-2]\rangle_j+|[1,1]\rangle_i|[-1,-1]\rangle_j+(i\leftrightarrow j))\\
&\quad+\frac{1}{\sqrt{40}}(7|[0,0]_1\rangle_i|[0,0]_1\rangle_j+3|[0,0]_2\rangle_i|[0,0]_2\rangle_j+2\sqrt{3}|[0,0]_1\rangle_i|[0,0]_2\rangle_j+2\sqrt{3}|[0,0]_2\rangle_i|[0,0]_1\rangle_j),
\end{aligned} \tag{C5}$$

where we use $|[p, q]\rangle_i$ to denote state $|(1, 1), (p, q)\rangle$ at site i for simplicity. Putting Eq. (C3) into Eq. (C5), we obtain Eq. (8) in the main text.

APPENDIX D: FLAVOR-WAVE THEORY

In this Appendix, we provide details for the flavor-wave theory [22–25]. In order to study low energy excitations, we assign three flavors of Shwinger bosons $a_{n\alpha}(j)$ at each site j on the nth sublattice, where $\alpha = x, y, z$ corresponds to x, y, z spin states defined in Eq. (B2). Here, $n = 1$ for the uniform states, while $n = 1, 2$ for the bipartite-lattice ordered states. Thus the operators $(\boldsymbol{S}, \boldsymbol{Q})$ can be written bilinearly in terms of Schwinger bosons,

$$S_n^\alpha(j) = -i\sum_{\beta\gamma}\epsilon_{\alpha\beta\gamma}a_{n\beta}^\dagger(j)a_{n\gamma}(j), \tag{D1a}$$

$$Q_n^{\mu\nu}(j)|_{\mu\neq\nu} = -[a_{n\mu}^\dagger(j)a_{n\nu}(j) + a_{n\nu}^\dagger(j)a_{n\mu}(j)], \tag{D1b}$$

$$Q_n^{x^2-y^2}(j) = -[a_{nx}^\dagger(j)a_{nx}(j) - a_{ny}^\dagger(j)a_{ny}(j)], \tag{D1c}$$

$$Q_n^{3z^2-r^2}(j) = -\frac{1}{\sqrt{3}}[3a_{nz}^\dagger(j)a_{nz}(j) - 1], \tag{D1d}$$

where the single occupancy constraint

$$\sum_\alpha a_{n\alpha}^\dagger(j)a_{n\alpha}(j) = 1 \tag{D2}$$

is imposed.

To obtain various spin ordered states, we shall condense these Schwinger bosons at some components. Without loss of generality, the condensate components are constructed by an SU(3) rotation Ω_n in the nth sublattice, which is defined as follows:

$$\begin{pmatrix} a_{n\tilde{x}} \\ a_{n\tilde{y}} \\ a_{n\tilde{z}} \end{pmatrix} = \Omega_n \begin{pmatrix} a_{nx} \\ a_{ny} \\ a_{nz} \end{pmatrix}. \tag{D3}$$

Such an SU(3) rotation Ω_n is site-independent and determined by corresponding mean-field $\boldsymbol{d}$ vectors and enable us to attribute the condensate to $a_{n\tilde{x}}$ component only. And $a_{n\tilde{y}}$ and $a_{n\tilde{z}}$ components are thought as small fractions. Then the low-energy Hamiltonian can be bilinearized by the Holstein-Primakoff transformation. Approximately, $a_{n\tilde{x}}^\dagger(j)$ and $a_{n\tilde{x}}(j)$ can be written as

$$a_{n\tilde{x}}^\dagger(j) = a_{n\tilde{x}}(j) = \sqrt{M - a_{n\tilde{y}}^\dagger(j)a_{n\tilde{y}}(j) - a_{n\tilde{z}}^\dagger(j)a_{n\tilde{z}}(j)}, \tag{D4}$$

where $M = 1$ in present case considering the single occupancy constraint.

Then we carry out the $1/M$ expansion in the Holstein-Primakoff bosons $a_{n\tilde{y}}$ and $a_{n\tilde{z}}$ up to quadratic order, and perform the Fourier transformation $a_{n\tilde{\alpha}}(\boldsymbol{k}) = \sum_j e^{i\boldsymbol{k}\cdot\vec{r}_j}a_{n\tilde{\alpha}}(j)/\sqrt{N}$ to obtain the Hamiltonian $\mathcal{H}$ in the k space, where $\vec{r}_j$ is the position of the lattice site j and N is the number of magnetic unit cells. Thus the k-space Hamiltonian can be diagonalized by the bosonic Bogoliubov transformation,

$$\mathcal{H} = \sum_{m,\boldsymbol{k}}\omega_m(\boldsymbol{k})b_m^\dagger(\boldsymbol{k})b_m(\boldsymbol{k}) + \mathcal{C}, \tag{D5}$$

where $\omega_m(\boldsymbol{k})$ is the energy dispersion of mth branch flavor wave, $b_m(\boldsymbol{k})$ and $b_m^\dagger(\boldsymbol{k})$ are bosonic Bogoliubov quasiparticle annihilation and creation operators, and the constant $\mathcal{C}$ does not depend on boson fields. For uniform states, say, FQ states, $m = 1,\ 2$; while for AFQ states, $m = 1,\ 2,\ 3,\ 4$. As long as the ground states of $\mathcal{H}$ determined by $K_1,\ K_2$ and K_3 are given, we are able to obtain the dispersions $\omega_m(\boldsymbol{k})$ simultaneously.

FQ1 phase. For FQ1 phase, the $\boldsymbol{d}$ vector of ground state reads $\boldsymbol{d}^{\mathrm{FQ1}} = \left(\begin{smallmatrix}1\\0\\0\end{smallmatrix}\right)$, and the global rotational matrix Ω^{FQ1} is a 3×3 unit matrix. We introduce the SU(3) Schwinger bosons as

$$\begin{pmatrix} a_{\tilde{x}} \\ a_{\tilde{y}} \\ a_{\tilde{z}} \end{pmatrix} = \begin{pmatrix} \sqrt{n_x} \\ a_y \\ a_z \end{pmatrix}, \tag{D6}$$

where

$$\sqrt{n_x} \equiv \sqrt{1 - a_y^\dagger a_y - a_z^\dagger a_z} \tag{D7}$$

Expanding spin dipolar and quadrupolar operators $\boldsymbol{S}$ and $\boldsymbol{Q}$ up to quadratic order of a_y and a_z gives rise to

$$\begin{aligned} S^x &= -i(a_y^\dagger a_z - a_z^\dagger a_y), \\ S^y &= -i(a_z^\dagger - a_z), \\ S^z &= i(a_y^\dagger - a_y), \\ Q^{xy} &= -(a_y^\dagger + a_y), \\ Q^{yz} &= -(a_y^\dagger a_z + a_z^\dagger a_y), \\ Q^{zx} &= -(a_z^\dagger + a_z), \\ Q^{x^2-y^2} &= -(1 - 2a_y^\dagger a_y - a_z^\dagger a_z), \\ Q^{3z^2-r^2} &= \frac{1}{\sqrt{3}}(3a_z^\dagger a_z - 1). \end{aligned} \tag{D8}$$

Put them into the Hamiltonian and keep all the terms up to quadratic order of a_y and a_z, we obtain

$$\mathcal{H}^{\mathrm{FQ1}} = \sum_{\boldsymbol{k}}\sum_{m=1}^{2}\omega_m^{\mathrm{FQ1}}(\boldsymbol{k})b_m^\dagger(\boldsymbol{k})b_m(\boldsymbol{k}), \tag{D9}$$

where

$$b_1(\boldsymbol{k}) = a_y(\boldsymbol{k}), \quad b_2(\boldsymbol{k}) = a_z(\boldsymbol{k}), \tag{D10}$$

Here, $\omega_{1,2}^{\mathrm{FQ1}}(\boldsymbol{k})$ are given in Table II in the main text. Note that all the spins condense at the $|x\rangle$ state. So that $b_1^\dagger = a_y^\dagger$ creates a $|y\rangle$ state and must annihilates an $|x\rangle$ state simultaneously to satisfy the single occupancy constraint in Eq. (D2). It means that the $\omega_1^{\mathrm{FQ1}}(\boldsymbol{k})$ mode corresponds to a two-magnon excitation. Similarly, $\omega_2^{\mathrm{FQ1}}(\boldsymbol{k})$ causes an $|x\rangle \to |z\rangle$ transition and is a one-magnon mode.

FQ2 phase. Considering the $\boldsymbol{d}$ vector of a FQ2 state being the form of $d^{\mathrm{FQ2}} = \left(\begin{smallmatrix}\cos\vartheta\\0\\\sin\vartheta\end{smallmatrix}\right)$ and the global rotational matrix

$$\Omega^{\mathrm{FQ2}} = \begin{pmatrix}\cos\vartheta & 0 & -\sin\vartheta\\ 0 & 1 & 0\\ \sin\vartheta & 0 & \cos\vartheta\end{pmatrix}, \tag{D11}$$

we introduce rotated Schwinger bosons as follows:

$$\begin{pmatrix}a_{\tilde{x}}\\ a_{\tilde{y}}\\ a_{\tilde{z}}\end{pmatrix} = \begin{pmatrix}\cos\vartheta\sqrt{n_x} - \sin\vartheta\, a_z\\ a_y\\ \sin\vartheta\sqrt{n_x} + \cos\vartheta\, a_z\end{pmatrix}, \tag{D12}$$

where $\sin\vartheta$ is determined by the mean-field theory and given in the caption in Table II in the main text. Similarly, the operators $(\boldsymbol{S}, \boldsymbol{Q})$ can be expanded to quadratic order of a_y and a_z as follows:

$$\begin{aligned}
S^x &= -i\sin\vartheta(a_y^\dagger - a_y) - i\cos\vartheta(a_y^\dagger a_z - a_z^\dagger a_y),\\
S^y &= -i(a_z^\dagger - a_z),\\
S^z &= i\cos\vartheta(a_y^\dagger - a_y) - i\sin\vartheta(a_y^\dagger a_z - a_z^\dagger a_y),\\
Q^{xy} &= -\cos\vartheta(a_y^\dagger + a_y) + \sin\vartheta(a_y^\dagger a_z + a_z^\dagger a_y),\\
Q^{yz} &= -\sin\vartheta(a_y^\dagger + a_y) + \sin\vartheta(a_y^\dagger a_z + a_z^\dagger a_y),\\
Q^{zx} &= (\sin^2\vartheta - \cos^2\vartheta)(a_z + a_z^\dagger)\\
&\quad - 2\sin\vartheta\cos\vartheta(1 - a_y^\dagger a_y - 2a_z^\dagger a_z),\\
Q^{x^2-y^2} &= -\cos^2\vartheta + \cos\vartheta\sin\vartheta(a_z + a_z^\dagger)\\
&\quad + (1 + \cos^2\vartheta)a_y^\dagger a_y + (2\cos^2\vartheta - 1)a_z^\dagger a_z,\\
Q^{3z^2-r^2} &= \sqrt{3}\cos^2\vartheta(a_z^\dagger a_z - \tan^2\vartheta(a_y^\dagger a_y + a_z^\dagger a_z))\\
&\quad + \frac{1}{\sqrt{3}}(3\sin\vartheta\cos\vartheta(a_z + a_z^\dagger) + 3\sin^2\vartheta - 1).
\end{aligned} \tag{D13}$$

Finally we obtain the diagonalized Hamiltonian

$$\mathcal{H}^{\mathrm{FQ2}} = \sum_{\boldsymbol{k}}\sum_{m=1}^{2}\omega_m^{\mathrm{FQ2}}(\boldsymbol{k})b_m^\dagger(\boldsymbol{k})b_m(\boldsymbol{k}), \tag{D14}$$

where $\omega_{1,2}^{\mathrm{FQ2}}(\boldsymbol{k})$ are given in Table II and the Bogoliubov transformation reads

$$\begin{aligned}
a_y(\boldsymbol{k}) &= b_1(\boldsymbol{k}),\\
a_z(\boldsymbol{k}) &= \cosh\left(\rho_{\boldsymbol{k}}^{\mathrm{FQ2}}\right)b_2(\boldsymbol{k}) + \sinh\left(\rho_{\boldsymbol{k}}^{\mathrm{FQ2}}\right)b_2^\dagger(-\boldsymbol{k}),
\end{aligned} \tag{D15}$$

with

$$\exp\left(\rho_{\boldsymbol{k}}^{\mathrm{FQ2}}\right) = \sqrt{\frac{1-\gamma(\boldsymbol{k})}{1+B_K\gamma(\boldsymbol{k})}}, \tag{D16}$$

where B_K and $\gamma(\boldsymbol{k})$ are given in Table II. In this case, condensate components are of $|x\rangle$ and $|z\rangle$ spins. Such that $\omega_2^{\mathrm{FQ2}}(\boldsymbol{k})$ mode corresponds to $|x\rangle \leftrightarrow |z\rangle$ transition, and is a one-magnon mode, while $\omega_1^{\mathrm{FQ2}}(\boldsymbol{k})$ mode corresponds to $|x\rangle + \tan\vartheta|z\rangle \leftrightarrow |y\rangle$ transition, and is an admixture of one-magnon and two-magnon modes.

FQ3 phase. Now the $\boldsymbol{d}$ vector is $\boldsymbol{d}^{\mathrm{FQ3}} = \left(\begin{smallmatrix}0\\0\\1\end{smallmatrix}\right)$, and the global rotational matrix reads

$$\Omega^{\mathrm{FQ3}} = \begin{pmatrix}0 & 0 & -1\\ 0 & 1 & 0\\ 1 & 0 & 0\end{pmatrix}. \tag{D17}$$

Then the rotated Schwinger bosons becomes

$$\begin{pmatrix}a_{\tilde{x}}\\ a_{\tilde{y}}\\ a_{\tilde{z}}\end{pmatrix} = \begin{pmatrix}-a_z\\ a_y\\ \sqrt{n_x}\end{pmatrix}. \tag{D18}$$

And the operators $\boldsymbol{S}$ and $\boldsymbol{Q}$ read

$$\begin{aligned}
S^x &= -i(a_y^\dagger - a_y),\\
S^y &= -i(a_z^\dagger - a_z),\\
S^z &= i(a_z^\dagger a_y - \mathrm{H.c.}),\\
Q^{xy} &= a_z^\dagger a_y + \mathrm{H.c.},\\
Q^{yz} &= -(a_y^\dagger + a_y),\\
Q^{zx} &= a_z^\dagger + a_z,\\
Q^{x^2-y^2} &= -(a_z^\dagger a_z - a_y^\dagger a_y),\\
Q_A^{3z^2-r^2} &= -\frac{1}{\sqrt{3}}(3a_y^\dagger a_y + 3a_z^\dagger a_z - 2).
\end{aligned} \tag{D19}$$

Putting them into the Hamiltonian, we obtain

$$\mathcal{H}^{\mathrm{FQ3}} = \sum_{\boldsymbol{k}}\sum_{m=1}^{2}\omega_m^{\mathrm{FQ3}}(\boldsymbol{k})b_m^\dagger(\boldsymbol{k})b_m(\boldsymbol{k}), \tag{D20}$$

where $\omega_{1,2}^{\mathrm{FQ3}}(\boldsymbol{k})$ are given in Table II and the Bogoliubov transformation reads

$$a_y(\boldsymbol{k}) = b_1(\boldsymbol{k}),\quad a_z(\boldsymbol{k}) = b_2(\boldsymbol{k}). \tag{D21}$$

In this case, the condensate component is $|z\rangle$. Such that $\omega_1^{\mathrm{FQ3}}(\boldsymbol{k})$ mode gives rise to $|z\rangle \to |y\rangle$ transition and is a one-magnon mode, and $\omega_2^{\mathrm{FQ3}}(\boldsymbol{k})$ mode gives rise to $|z\rangle \leftrightarrow |x, y\rangle$ transition and is a one-magnon mode too.

AFQ1 phase. The $\boldsymbol{d}$ vectors in sublattices 1 and 2 are of the form $\boldsymbol{d}_1^{\mathrm{AFQ1}} = \left(\begin{smallmatrix}1\\0\\0\end{smallmatrix}\right)$, $\boldsymbol{d}_2^{\mathrm{AFQ1}} = \left(\begin{smallmatrix}0\\1\\0\end{smallmatrix}\right)$, and the corresponding global rotational matrices Ω_1^{AFQ1} and Ω_2^{AFQ1} read

$$\Omega_1^{\mathrm{AFQ1}} = \begin{pmatrix}1 & 0 & 0\\ 0 & 1 & 0\\ 0 & 0 & 1\end{pmatrix},\quad \Omega_2^{\mathrm{AFQ1}} = \begin{pmatrix}0 & -1 & 0\\ 1 & 0 & 0\\ 0 & 0 & 1\end{pmatrix}. \tag{D22}$$

Therefore the SU(3) Schwinger bosons in the rotated representation can be written as

$$\begin{aligned}
\begin{pmatrix}a_{1\tilde{x}}\\ a_{1\tilde{y}}\\ a_{1\tilde{z}}\end{pmatrix} &= \begin{pmatrix}\sqrt{n_{1x}}\\ a_{1y}\\ a_{1z}\end{pmatrix},\\
\begin{pmatrix}a_{2\tilde{x}}\\ a_{2\tilde{y}}\\ a_{2\tilde{z}}\end{pmatrix} &= \begin{pmatrix}-a_{2y}\\ \sqrt{n_{2x}}\\ a_{2z}\end{pmatrix},
\end{aligned} \tag{D23}$$

where $\sqrt{n_{mx}} = \sqrt{1 - a_{my}^\dagger a_{my} - a_{mz}^\dagger a_{mz}}$ for $m = 1$ and 2. Expanding $(\boldsymbol{S}, \boldsymbol{Q})$ to quadratic order of a_{my} and a_{mz} in each sublattice gives rise to

$$\begin{aligned}
S_1^x &= -i(a_{1y}^\dagger a_{1z} - a_{1z}^\dagger a_{1y}), \quad S_2^x = i(a_{2z}^\dagger - a_{2z}),\\
S_1^y &= -i(a_{1z}^\dagger - a_{1z}), \quad S_2^y = -i(a_{2y}^\dagger a_{2z} - a_{2z}^\dagger a_{2y}),\\
S_1^z &= i(a_{1y}^\dagger - a_{1y}), \quad S_2^z = i(a_{2y}^\dagger - a_{2y}),\\
Q_1^{xy} &= -(a_{1y}^\dagger + a_{1y}), \quad Q_2^{xy} = (a_{2y}^\dagger + a_{2y}),\\
Q_1^{yz} &= -(a_{1y}^\dagger a_{1z} + a_{1z}^\dagger a_{1y}), \quad Q_2^{yz} = -(a_{2z}^\dagger + a_{2z}),\\
Q_1^{zx} &= -(a_{1z}^\dagger + a_{1z}), \quad Q_2^{zx} = (a_{2y}^\dagger a_{2z} + 2_{2z}^\dagger 2_{2y}),\\
Q_1^{x^2-y^2} &= -(1 - 2a_{1y}^\dagger a_{1y} - a_{1z}^\dagger a_{1z}),\\
Q_2^{x^2-y^2} &= (1 - 2a_{2y}^\dagger a_{2y} - a_{2z}^\dagger a_{2z}),\\
Q_1^{3z^2-r^2} &= \frac{1}{\sqrt{3}}(3a_{1z}^\dagger a_{1z} - 1),\\
Q_2^{3z^2-r^2} &= \frac{1}{\sqrt{3}}(3a_{2z}^\dagger a_{2z} - 1).
\end{aligned} \tag{D24}$$

Then the mean-field Hamiltonian of AFQ1 becomes

$$\mathcal{H}^{\text{AFQ1}} = \sum_{\boldsymbol{k}} \sum_{m=1}^{4} \omega_m^{\text{AFQ1}}(\boldsymbol{k}) b_m^\dagger(\boldsymbol{k}) b_m(\boldsymbol{k}), \tag{D25}$$

where $\omega_{1,2}^{\text{FQ1}}(\boldsymbol{k})$ are given in Table II in the main text. The Bogoliubov transformation reads

$$\begin{aligned}
&a_{1z}(\boldsymbol{k}) = b_3(\boldsymbol{k}), \quad a_{2z}(\boldsymbol{k}) = b_4(\boldsymbol{k}),\\
&\begin{pmatrix} a_{1y}(\boldsymbol{k}) \\ a_{2y}(\boldsymbol{k}) \end{pmatrix} = \begin{pmatrix} c_{\boldsymbol{k}}^{\text{A1}} & c_{\boldsymbol{k}}^{\text{A1}} & s_{\boldsymbol{k}}^{\text{A1}} & -s_{\boldsymbol{k}}^{\text{A1}} \\ c_{\boldsymbol{k}}^{\text{A1}} & -c_{\boldsymbol{k}}^{\text{A1}} & s_{\boldsymbol{k}}^{\text{A1}} & s_{\boldsymbol{k}}^{\text{A1}} \end{pmatrix} \begin{pmatrix} b_1(\boldsymbol{k}) \\ b_2(\boldsymbol{k}) \\ b_1^\dagger(-\boldsymbol{k}) \\ b_2^\dagger(-\boldsymbol{k}) \end{pmatrix},
\end{aligned} \tag{D26}$$

with

$$c_{\boldsymbol{k}}^{\text{A1}} \equiv \frac{1}{\sqrt{2}} \cosh\left(\rho_{\boldsymbol{k}}^{\text{A1}}\right), \quad s_{\boldsymbol{k}}^{\text{A1}} \equiv \frac{1}{\sqrt{2}} \sinh\left(\rho_{\boldsymbol{k}}^{\text{A1}}\right), \tag{D27}$$

and $\rho_{\boldsymbol{k}}^{\text{A1}}$ is given as

$$\exp\left(2\rho_{\boldsymbol{k}}^{\text{A1}}\right) = \sqrt{\frac{1+\gamma(\boldsymbol{k})}{1-\gamma(\boldsymbol{k})}}. \tag{D28}$$

Similar to the case of FQ1, all the spins condense at the $|x\rangle$ state. So that $\omega_{1,2}^{\text{AFQ1}}(\boldsymbol{k})$ modes give rise to $|x\rangle \rightarrow |y\rangle$ transitions and correspond to two-magnon excitations. And $\omega_{3,4}^{\text{AFQ1}}(\boldsymbol{k})$ modes give rise to $|x\rangle \leftrightarrow |z\rangle$ transition and are one-magnon excitations.

AFQ2 phase. In this phase, the $\boldsymbol{d}$ vectors in two sublattice are $d_1^{\text{AFQ2}} = \left(\begin{smallmatrix} \cos\vartheta \\ 0 \\ \sin\vartheta \end{smallmatrix}\right)$ and $d_2^{\text{AFQ2}} = \left(\begin{smallmatrix} \cos\vartheta \\ 0 \\ -\sin\vartheta \end{smallmatrix}\right)$, and the global rotational matrices read

$$\begin{aligned}
\Omega_1^{\text{AFQ2}} &= \begin{pmatrix} \cos\vartheta & 0 & -\sin\vartheta \\ 0 & 1 & 0 \\ \sin\vartheta & 0 & \cos\vartheta \end{pmatrix},\\
\Omega_1^{\text{AFQ2}} &= \begin{pmatrix} \cos\vartheta & 0 & \sin\vartheta \\ 0 & 1 & 0 \\ -\sin\vartheta & 0 & \cos\vartheta \end{pmatrix}.
\end{aligned} \tag{D29}$$

We have SU(3) Schwinger bosons in such rotated representation as follows:

$$\begin{aligned}
\begin{pmatrix} a_{1\tilde{x}} \\ a_{1\tilde{y}} \\ a_{1\tilde{z}} \end{pmatrix} &= \begin{pmatrix} \cos\vartheta\sqrt{n_{1x}} - \sin\vartheta\, a_{1z} \\ a_{1y} \\ \sin\vartheta\sqrt{n_{1x}} + \cos\vartheta\, a_{1z} \end{pmatrix},\\
\begin{pmatrix} a_{2\tilde{x}} \\ a_{2\tilde{y}} \\ a_{2\tilde{z}} \end{pmatrix} &= \begin{pmatrix} \cos\vartheta\sqrt{n_{2x}} + \sin\vartheta\, a_{2z} \\ a_{2y} \\ -\sin\vartheta\sqrt{n_{2x}} + \cos\vartheta\, a_{2z} \end{pmatrix}.
\end{aligned} \tag{D30}$$

Then the forms of $(\boldsymbol{S}, \boldsymbol{Q})$ for each sublattice of AFQ2 are very similar to Eq. (D13), and here we do not list them explicitly.

The corresponding Hamiltonian becomes

$$\mathcal{H}^{\text{AFQ2}} = \sum_{\boldsymbol{k}} \sum_{m=1}^{4} \omega_m^{\text{AFQ2}}(\boldsymbol{k}) b_m^\dagger(\boldsymbol{k}) b_m(\boldsymbol{k}), \tag{D31}$$

where $\omega_{1,2,3,4}^{\text{AFQ2}}$ are given in Table II in the main text. The Bogoliubov transformation are chosen as

$$\begin{pmatrix} a_{1y}(\boldsymbol{k}) \\ a_{2y}(\boldsymbol{k}) \end{pmatrix} = \frac{1}{\sqrt{2}} \begin{pmatrix} 1 & 1 \\ 1 & -1 \end{pmatrix} \begin{pmatrix} b_1(\boldsymbol{k}) \\ b_2(\boldsymbol{k}) \end{pmatrix} \tag{D32}$$

and

$$\begin{pmatrix} a_{1z}(\boldsymbol{k}) \\ a_{2z}(\boldsymbol{k}) \end{pmatrix} = \begin{pmatrix} c_{1\boldsymbol{k}}^{\text{A2}} & c_{2\boldsymbol{k}}^{\text{A2}} & s_{1\boldsymbol{k}}^{\text{A2}} & s_{2\boldsymbol{k}}^{\text{A2}} \\ c_{1\boldsymbol{k}}^{\text{A2}} & -c_{2\boldsymbol{k}}^{\text{A2}} & s_{1\boldsymbol{k}}^{\text{A2}} & -s_{2\boldsymbol{k}}^{\text{A2}} \end{pmatrix} \begin{pmatrix} b_3(\boldsymbol{k}) \\ b_4(\boldsymbol{k}) \\ b_3^\dagger(-\boldsymbol{k}) \\ b_4^\dagger(-\boldsymbol{k}) \end{pmatrix}, \tag{D33}$$

where

$$c_{m\boldsymbol{k}}^{\text{A2}} \equiv \frac{1}{\sqrt{2}} \cosh\left(\rho_{m\boldsymbol{k}}^{\text{A2}}\right), \quad s_{m\boldsymbol{k}}^{\text{A2}} \equiv \frac{1}{\sqrt{2}} \sinh\left(\rho_{m\boldsymbol{k}}^{\text{A2}}\right), \tag{D34}$$

with $m = 1$ and 2 and

$$\begin{aligned}
\exp\left(2\rho_{1\boldsymbol{k}}^{\text{A2}}\right) &= \sqrt{\frac{1+\gamma(\boldsymbol{k})}{1-B_K\gamma(\boldsymbol{k})}},\\
\exp\left(2\rho_{2\boldsymbol{k}}^{\text{A2}}\right) &= \sqrt{\frac{1-\gamma(\boldsymbol{k})}{1+B_K\gamma(\boldsymbol{k})}}.
\end{aligned} \tag{D35}$$

Similar to the case of FQ2, in this case condensate components are of $|x\rangle$ and $|z\rangle$ spins. So $\omega_{3,4}^{\text{AFQ2}}(\boldsymbol{k})$ modes which correspond to $|x\rangle \leftrightarrow |z\rangle$ transition are one-magnon modes, while $\omega_{1,2}^{\text{AFQ2}}(\boldsymbol{k})$ modes correspond to $|x\rangle \pm \tan\vartheta|z\rangle \leftrightarrow |y\rangle$ transitions, and are admixtures of one-magnon and two-magnon modes.

AFQ3 phase. The AFQ3 ground states are given by the d-vectors in two sublattices as the following, $\boldsymbol{d}_1^{\text{AFQ3}} = \left(\begin{smallmatrix} 0 \\ 0 \\ 1 \end{smallmatrix}\right)$, $\boldsymbol{d}_2^{\text{AFQ3}} = \left(\begin{smallmatrix} 1 \\ 0 \\ 0 \end{smallmatrix}\right)$. Now the global rotational matrices Ω_1^{AFQ3} and Ω_2^{AFQ3} read,

$$\Omega_1^{\text{AFQ3}} = \begin{pmatrix} 0 & 0 & -1 \\ 0 & 1 & 0 \\ 1 & 0 & 0 \end{pmatrix}, \quad \Omega_2^{\text{AFQ3}} = \begin{pmatrix} 1 & 0 & 0 \\ 0 & 1 & 0 \\ 0 & 0 & 1 \end{pmatrix}. \tag{D36}$$

The corresponding Schwinger bosons in the rotated representations are

$$\begin{pmatrix} a_{1\tilde{x}} \\ a_{2\tilde{y}} \\ a_{3\tilde{z}} \end{pmatrix} = \begin{pmatrix} -a_{1z} \\ a_{1y} \\ \sqrt{n_{1x}} \end{pmatrix},$$

$$\begin{pmatrix} a_{2\tilde{x}} \\ a_{2\tilde{y}} \\ a_{2\tilde{z}} \end{pmatrix} = \begin{pmatrix} \sqrt{n_{2x}} \\ a_{2y} \\ a_{2z} \end{pmatrix}. \tag{D37}$$

And operators $(\boldsymbol{S}, \boldsymbol{Q})$ for each sublattice read

$$\begin{aligned}
S_1^x &= -i(a_{1y}^\dagger - a_{1y}), \quad S_2^x = -i(a_{2y}^\dagger a_{2z} - a_{2z}^\dagger a_{2y}),\\
S_1^y &= -i(a_{1z}^\dagger - a_{1z}), \quad S_2^y = -i(a_{2z}^\dagger - a_{2z}),\\
S_1^z &= i(a_{1z}^\dagger a_{1y} - a_{1y}^\dagger a_{1z}), \quad S_2^z = i(a_{2y}^\dagger - a_{2y}),\\
Q_1^{xy} &= a_{1z}^\dagger a_{1y} + a_{1y}^\dagger a_{1z}, \quad Q_2^{xy} = -(a_{2y}^\dagger + a_{2y}),\\
Q_1^{yz} &= -(a_{1y}^\dagger + a_{1y}), \quad Q_2^{yz} = -(a_{2y}^\dagger a_{2z} + a_{2z}^\dagger a_{2y}),\\
Q_1^{zx} &= a_{1z}^\dagger + a_{1z}, \quad Q_2^{zx} = -(a_{2z}^\dagger + a_{2z}),\\
Q_1^{x^2-y^2} &= -(a_{1z}^\dagger a_{1z} - a_{1y}^\dagger a_{1y}),\\
Q_2^{x^2-y^2} &= -(1 - 2a_{2y}^\dagger a_{2y} - a_{2z}^\dagger a_{2z}),\\
Q_1^{3z^2-r^2} &= -\frac{1}{\sqrt{3}}(3a_{1z}^\dagger a_{1z} + 3a_{1y}^\dagger a_{1y} - 2),\\
Q_2^{3z^2-r^2} &= -\frac{1}{\sqrt{3}}(1 - 3a_{2z}^\dagger a_{2z}).
\end{aligned} \tag{D38}$$

The diagonolized Hamiltonian reads

$$\mathcal{H}^{\mathrm{AFQ3}} = \sum_{\boldsymbol{k}} \sum_{m=1}^{4} \omega_m^{\mathrm{AFQ3}}(\boldsymbol{k}) b_m^\dagger(\boldsymbol{k}) b_m(\boldsymbol{k}). \tag{D39}$$

where $\omega_{1,2,3,4}^{\mathrm{AFQ3}}$ are given in Table II and

$$a_{1y}(\boldsymbol{k}) = b_1(\boldsymbol{k}), \qquad a_{2y}(\boldsymbol{k}) = b_2(\boldsymbol{k}),$$

$$\begin{pmatrix} a_{1z}(\boldsymbol{k}) \\ a_{2z}^\dagger(-\boldsymbol{k}) \end{pmatrix} = \begin{pmatrix} \cosh\left(\rho_{\boldsymbol{k}}^{\mathrm{A3}}\right) & \sinh\left(\rho_{\boldsymbol{k}}^{\mathrm{A3}}\right) \\ \sinh\left(\rho_{\boldsymbol{k}}^{\mathrm{A3}}\right) & \cosh\left(\rho_{\boldsymbol{k}}^{\mathrm{A3}}\right) \end{pmatrix} \begin{pmatrix} b_3(\boldsymbol{k}) \\ b_4^\dagger(-\boldsymbol{k}) \end{pmatrix}. \tag{D40}$$

Here,

$$\exp\left(2\rho_{\boldsymbol{k}}^{\mathrm{A3}}\right) = \sqrt{\frac{3K_3 + K_1 - 4K_2\gamma(\boldsymbol{k})}{3K_3 + K_1 + 4K_2\gamma(\boldsymbol{k})}}. \tag{D41}$$

In this case, all spins condense at the $|x\rangle$ state. Thus $\omega_{1,2}^{\mathrm{AFQ3}}(\boldsymbol{k})$ modes corresponding to $|x\rangle \leftrightarrow |y\rangle$ transitions are two-magnon modes. While $\omega_{3,4}^{\mathrm{AFQ3}}(\boldsymbol{k})$ modes corresponding to $|x\rangle \leftrightarrow |z\rangle$ transitions are one-magnon modes.

APPENDIX E: SPECTRAL FUNCTIONS

We provide details for spin spectral function $S(\boldsymbol{q}, \omega)$ and spin quardrupole spectral function $Q(\boldsymbol{q}, \omega)$, which are calculated by the linearized flavor-wave theory.

1. Spin spectral functions

In this section, we demonstrate details for $S(\boldsymbol{q}, \omega)$.

FQ1 phase. The spin operators in the flavor-wave theory read

$$\begin{aligned}
S^x &= (r_1 - ir_2)a_z + (r_1 + ir_2)a_z^\dagger,\\
S^y &= (-r_3 - ir_0)a_z + (-r_3 + ir_0)a_z^\dagger,\\
S^z &= ua_y + u^* a_y^\dagger,
\end{aligned} \tag{E1}$$

where

$$u = i(r_0 - ir_3)^2 + i(r_2 + ir_1)^2, \tag{E2}$$

and the quadratic boson and constant terms are omitted. Note that the constant does not contribute to any excitations thereby the spectral functions. Then spin spectral function reads

$$S_{\mathrm{FQ1}}(\boldsymbol{q}, \omega) = 2\pi\left[\delta\left(\omega - \omega_2^{\mathrm{FQ1}}(\boldsymbol{q})\right) + |u|^2\delta\left(\omega - \omega_1^{\mathrm{FQ1}}(\boldsymbol{q})\right)\right]. \tag{E3}$$

AFQ1 phase. The spin operators for sublattice 1 are the same as Eq. (E1) but with additional sublattice subindex and the spin operators for sublattice 2 read

$$\begin{aligned}
S_2^x &= (ir_0 - r_3)a_{2z} + (-ir_0 - r_3)a_{2z}^\dagger,\\
S_2^y &= (-r_1 - ir_2)a_{2z} + (-r_1 + ir_2)a_{2z}^\dagger,\\
S_2^z &= -u^* a_{2y} - ua_{2y}^\dagger.
\end{aligned} \tag{E4}$$

And spin spectral function is

$$S_{\mathrm{AFQ1}}(\boldsymbol{q}, \omega) = 2\pi\delta\left(\omega - \omega_3^{\mathrm{AFQ1}}(\boldsymbol{q})\right) + 2\pi\sqrt{\frac{1-\gamma(\boldsymbol{q})}{1+\gamma(\boldsymbol{q})}}|u|^2\delta\left(\omega - \omega_1^{\mathrm{AFQ1}}(\boldsymbol{q})\right), \tag{E5}$$

where u is defined in Eq. (E2).

FQ2 phase. The spin operators read

$$\begin{aligned}
S^x &= (-ir_2 + r_1\cos 2\vartheta)a_z - \sin\vartheta(r_3 + ir_0)a_y + \mathrm{H.c.},\\
S^y &= (-ir_0 - r_3\cos 2\vartheta)a_z - \sin\vartheta(r_1 - ir_2)a_y + \mathrm{H.c.},\\
S^z &= u\cos\vartheta\, a_y + (r_0 r_1 + r_2 r_3)\sin 2\vartheta\, a_z + \mathrm{H.c.}
\end{aligned} \tag{E6}$$

And spin spectral function reads

$$S_{\mathrm{FQ2}}(\boldsymbol{q}, \omega) = 2\pi F_1(\vartheta, \hat{r})\delta\left(\omega - \omega_1^{\mathrm{FQ2}}(\boldsymbol{q})\right) + 2\pi F_2(\vartheta, \hat{r})\sqrt{\frac{1 + B_K\gamma(\boldsymbol{q})}{1-\gamma(\boldsymbol{q})}}\delta\left(\omega - \omega_2^{\mathrm{FQ2}}(\boldsymbol{q})\right), \tag{E7}$$

where u is defined in Eq. (E2) and

$$\begin{aligned}
F_1(\vartheta, \hat{r}) &= 1 + (|u|^2 - 1)\cos^2\vartheta,\\
F_2(\vartheta, \hat{r}) &= 1 + \frac{4r_0^2 + 4r_2^2 - 3 - |u|^2}{4}\sin^2 2\vartheta.
\end{aligned} \tag{E8}$$

AFQ2 phase. The forms of spin operators for sublattice 1 are the same as Eq. (E6). And for sublattice 2 we can obtain spin operators by taking $\vartheta \to -\vartheta$. So here we do not list them explicitly. The dipolar spin spectral function reads

$$S_{\mathrm{AFQ2}}(\boldsymbol{q},\omega) = 2\pi\sin^2\vartheta\,\delta(\omega-\omega_2^{\mathrm{AFQ2}}(\boldsymbol{q})) + 2\pi|u|^2\cos^2\vartheta\,\delta(\omega-\omega_1^{\mathrm{AFQ2}}(\boldsymbol{q})) + 2\pi(r_0^2+r_2^2)\sqrt{\frac{1-B_K\gamma(\boldsymbol{q})}{1+\gamma(\boldsymbol{q})}}\delta(\omega-\omega_3^{\mathrm{AFQ2}}(\boldsymbol{q})) + 2\pi(r_1^2+r_3^2)\cos^2 2\vartheta\sqrt{\frac{1+\gamma(\boldsymbol{q})}{1-B_K\gamma(\boldsymbol{q})}}\delta(\omega-\omega_3^{\mathrm{AFQ2}}(\boldsymbol{q})) + \pi\frac{(1-|u|^2)\sin^2 2\vartheta}{2}\sqrt{\frac{1-\gamma(\boldsymbol{q})}{1+B_K\gamma(\boldsymbol{q})}}\delta(\omega-\omega_4^{\mathrm{FQ2}}(\boldsymbol{q})), \tag{E9}$$

where u is defined in Eq. (E2).

FQ3 phase. The spin operators are

$$S^x = (ir_0+r_3)a_y + (r_1+ir_2)a_z + \mathrm{H.c.}, \quad S^y = (ir_0-r_3)a_z + (r_1-ir_2)a_y + \mathrm{H.c.}, \quad S^z = 0. \tag{E10}$$

And the dipolar spin spectral function reads

$$S_{\mathrm{FQ3}}(\boldsymbol{q},\omega) = 2\pi[\delta(\omega-\omega_1^{\mathrm{FQ3}}(\boldsymbol{q})) + \delta(\omega-\omega_2^{\mathrm{FQ3}}(\boldsymbol{q}))], \tag{E11}$$

Note that $S_{\mathrm{FQ3}}(\boldsymbol{q},\omega)$ does not depend on the $\boldsymbol{d}$ vector.

AFQ3 phase. The forms of spin operators for sublattice 1(2) are the same as Eq. (E10) [Eq. (E1)] with additional sublattice index. Thus the dipolar spin spectral function for an AFQ3 state does not depend on the $\boldsymbol{d}$ vector as well and reads

$$S_{\mathrm{AFQ3}}(\boldsymbol{q},\omega) = \pi\delta(\omega-\omega_1^{\mathrm{AFQ3}}(\boldsymbol{q})) + \pi\sqrt{\frac{C_K-D_K\gamma(\boldsymbol{q})}{C_K+D_K\gamma(\boldsymbol{q})}}\delta(\omega-\omega_3^{\mathrm{AFQ3}}(\boldsymbol{q})) + \pi\sqrt{\frac{C_K-D_K\gamma(\boldsymbol{q})}{C_K+D_K\gamma(\boldsymbol{q})}}\delta(\omega-\omega_4^{\mathrm{AFQ3}}(\boldsymbol{q})). \tag{E12}$$

2. Quadrupole spectral functions

In this section, we demonstrate details for $Q(\boldsymbol{q},\omega)$.

FQ1 phase. The $\boldsymbol{Q}$ operators read

$$Q^{xy} = va_z + \mathrm{H.c.}, \quad Q^{yz} = (r_2+ir_1)a_z + \mathrm{H.c.}, \quad Q^{zx} = (ir_3-r_0)a_z + \mathrm{H.c.}, \quad Q^{3z^2-r^2} = 0, \quad Q^{x^2-y^2} = 2(ir_3-r_0)(r_2+ir_1)a_y + \mathrm{H.c.}, \tag{E13}$$

where

$$v = (ir_0+r_2)^2 - (ir_3-r_0)^2. \tag{E14}$$

Notice the r_is are defined in Eq. (10) and again the quadratic boson and constant terms are omitted. Then the quadrupolar spin spectral function reads

$$Q_{\mathrm{FQ1}}(\boldsymbol{q},\omega) = 2\pi\delta(\omega-\omega_2^{\mathrm{FQ1}}(\boldsymbol{q})) + 2\pi(2-|u|^2)\delta(\omega-\omega_1^{\mathrm{FQ1}}(\boldsymbol{q})), \tag{E15}$$

where u is defined in Eq. (E2).

AFQ1 phase. The $\boldsymbol{Q}$ operators for sublattice 1 are the same as Eq. (E13) but with additional sublattice subindex and the $\boldsymbol{Q}$ operators for sublattice 2 read

$$Q_2^{xy} = -v^*a_{2z} + \mathrm{H.c.}, \quad Q_2^{yz} = -(r_0+ir_3)a_{2z} + \mathrm{H.c.}, \quad Q_2^{zx} = (ir_1-r_2)a_{2z} + \mathrm{H.c.}, \quad Q_2^{3z^2-r^2} = 0, \quad Q_2^{x^2-y^2} = 2(ir_3+r_0)(r_2-ir_1)a_{2y} + \mathrm{H.c.}, \tag{E16}$$

where v is defined in Eq. (E14). The quadrupolar spin spectral function is

$$Q_{\mathrm{AFQ1}}(\boldsymbol{q},\omega) = 2\pi\delta(\omega-\omega_3^{\mathrm{AFQ1}}(\boldsymbol{q})) + 2\pi(2-|u|^2)\sqrt{\frac{1-\gamma(\boldsymbol{q})}{1+\gamma(\boldsymbol{q})}}\delta(\omega-\omega_1^{\mathrm{AFQ1}}(\boldsymbol{q})), \tag{E17}$$

where u is defined in Eq. (E2).

FQ2 phase. The $\boldsymbol{Q}$ operators read

$$Q^{xy} = v\cos\vartheta\,a_y - (r_0r_2 - r_1r_3)\sin 2\vartheta\,a_z + \mathrm{H.c.}, \quad Q^{zx} = (ir_3 - r_0\cos 2\vartheta)a_z - \sin\vartheta(ir_1+r_2)a_y + \mathrm{H.c.}, \quad Q^{yz} = (ir_1 + r_2\cos 2\vartheta)a_z + \sin\vartheta(ir_3-r_0)a_y + \mathrm{H.c.}, \quad Q^{x^2-y^2} = (1/2 - r_1^2 - r_2^2)\sin 2\vartheta\,a_z + 2\cos\vartheta(ir_1+r_2)(ir_3-r_0)a_y + \mathrm{H.c.}, \quad Q^{3z^2-r^2} = \sqrt{3}\sin 2\vartheta\,a_z/2 + \mathrm{H.c.} \tag{E18}$$

where v is defined in Eq. (E14). And quadrupolar spin spectral function reads

$$Q_{\mathrm{FQ2}}(\boldsymbol{q},\omega) = 2\pi F_3(\vartheta,\hat{r})\delta(\omega-\omega_1^{\mathrm{FQ2}}(\boldsymbol{q})) + 2\pi F_4(\vartheta,\hat{r})\sqrt{\frac{1+B_K\gamma(\boldsymbol{q})}{1-\gamma(\boldsymbol{q})}}\delta(\omega-\omega_2^{\mathrm{FQ2}}(\boldsymbol{q})), \tag{E19}$$

where u is defined in Eq. (E2) and

$$F_3(\vartheta,\hat{r}) = 1 + (1-|u|^2)\cos^2\vartheta, \quad F_4(\vartheta,\hat{r}) = 1 + \frac{4r_1^2 + 4r_3^2 - 1 + |u|^2}{4}\sin^2 2\vartheta. \tag{E20}$$

AFQ2 phase. The forms of $\boldsymbol{Q}$ operators for sublattice 1 are the same as Eq. (E18). And for sublattice 2 we can obtain the $\boldsymbol{Q}$ operators by taking $\vartheta \to -\vartheta$. The quadrupolar spin spectral function reads

$$Q_{\mathrm{AFQ2}}(\boldsymbol{q},\omega) = 2\pi\sin^2\vartheta\,\delta(\omega-\omega_2^{\mathrm{AFQ2}}(\boldsymbol{q})) + 2\pi(2-|u|^2)\cos^2\vartheta\,\delta(\omega-\omega_1^{\mathrm{AFQ2}}(\boldsymbol{q})) + 2\pi(r_1^2+r_3^2)\sqrt{\frac{1-B_K\gamma(\boldsymbol{q})}{1+\gamma(\boldsymbol{q})}}\delta(\omega-\omega_3^{\mathrm{AFQ2}}(\boldsymbol{q}))$$

$$+\ 2\pi\left(r_0^2+r_2^2\right)\cos^2 2\vartheta\sqrt{\frac{1+\gamma(\boldsymbol{q})}{1-B_K\gamma(\boldsymbol{q})}}\delta\left(\omega-\omega_3^{\mathrm{AFQ2}}(\boldsymbol{q})\right)$$
$$+\ \pi\frac{(3+|u|^2)\sin^2 2\vartheta}{2}\sqrt{\frac{1-\gamma(\boldsymbol{q})}{1+B_K\gamma(\boldsymbol{q})}}\delta\left(\omega-\omega_4^{\mathrm{FQ2}}(\boldsymbol{q})\right), \quad \text{(E21)}$$

where u is defined in Eq. (E2).

FQ3 phase. The $\boldsymbol{Q}$ operators are

$$Q^{xy}=Q^{x^2-y^2}=Q^{3z^2-r^2}=0,$$
$$Q^{yz}=(ir_1-r_2)a_z+(ir_3-r_0)a_y+\text{H.c.},$$
$$Q^{zx}=(ir_3+r_0)a_z-(ir_1+r_2)a_y+\text{H.c.} \quad \text{(E22)}$$

And the quadrupolar spin spectral function $Q_{\mathrm{FQ3}}(\boldsymbol{q},\omega)$ is the same as Eq. (E11) and does not depend on the $\boldsymbol{d}$ vector.

AFQ3 phase. The forms of $\boldsymbol{Q}$ operators for sublattice 1(2) are the same as Eq. (E22) [Eq. (E13)] with additional sublattice index. Thus the quadrupolar spin spectral function $Q_{\mathrm{AFQ3}}(\boldsymbol{q},\omega)$ is the same as Eq. (E12). and does not depend on the $\boldsymbol{d}$ vector.

APPENDIX F: CONNECTION WITH t-J-V MODEL

Finally, we would like to point out that the SU(2) × $U(1)$ model can be mapped to the t-J-V model in one dimension, which is exactly solvable in the supersymmetric point [39,40]. We use S_γ to denote the effective spin for SU$(2)_\gamma$ symmetry. Then the local spin state $|z\rangle$ is SU$(2)_\gamma$ invariant and belongs to SU$(2)_\gamma$ irreducible representation (IR) $S_\gamma=0$, while $|x\rangle$ and $|y\rangle$ belong to SU$(2)_\gamma$ IR $S_\gamma=\frac{1}{2}$. Therefore $|z\rangle$ can be treat as a "hole" state, and the SU(2) × $U(1)$ symmetric model defined in Eq. (9) can be mapped to the t-J-V model, which reads [8,9,41]

$$H=-t\sum_{j,a}P\psi_{j,a}^\dagger\psi_{j+1,a}P+\text{H.c.}$$
$$+\sum_j P(J\vec{s}_j\cdot\vec{s}_{j+1}+Vn_jn_{j+1})P, \quad \text{(F1)}$$

where P projects out states with double occupancy and electron spin $\vec{s}_j$ and n_j on site j are defined as

$$\vec{s}_j\equiv\sum_{a,b}\psi_{j,a}^\dagger\vec{\sigma}_{ab}\psi_{j,b},\ n_j\equiv\sum_a\psi_{j,a}^\dagger\psi_{j,a}. \quad \text{(F2)}$$

The spin-1/2 indices, $a,b=\uparrow,\downarrow$. Letting $|\uparrow\rangle$ and $|\downarrow\rangle$ correspond to $|x\rangle$ and $|y\rangle$, and the "hole" state correspond to $|z\rangle$ in spin-1 system, we can establish a mapping form the t-J-V model to the SU(2) × $U(1)$ model defined in Eq. (9) through

$$K_1=J/4,\ K_2=t/2,\ K_3=V/3. \quad \text{(F3)}$$

Hamiltonian given in Eq. (F1) is equivalent to the SU(3) symmetric model when $J=2t$ and $V=3t/2$. And the supersymmetric t-J-V model can be realized when $K_1=K_2=-K_3/3$.

[1] F. D. M. Haldane, Phys. Rev. Lett. **50**, 1153 (1983).
[2] X. Chen, Z.-C. Gu, and X.-G. Wen, Phys. Rev. B **82**, 155138 (2010).
[3] F. Pollmann, A. M. Turner, E. Berg, and M. Oshikawa, Phys. Rev. B **81**, 064439 (2010).
[4] X. Chen, Z.-C. Gu, and X.-G. Wen, Phys. Rev. B **83**, 035107 (2011).
[5] Z.-X. Liu, M. Liu, and X.-G. Wen, Phys. Rev. B **84**, 075135 (2011).
[6] Z.-X. Liu, Y. Zhou, and T.-K. Ng, Phys. Rev. B **81**, 224417 (2010).
[7] G. V. Uimin, Pis'ma v Zh. Eksp. Teor. Fiz. **12**, 332 (1970) [JETP Lett. **12**, 225 (1970)].
[8] C. K. Lai, J. Math. Phys. **15**, 1675 (1974).
[9] B. Sutherland, Phys. Rev. B **12**, 3795 (1975).
[10] G. Fáth and J. Sólyom, Phys. Rev. B **51**, 3620 (1995).
[11] A. Läuchli, G. Schmid, and S. Trebst, Phys. Rev. B **74**, 144426 (2006).
[12] S. R. Manmana, A. M. Läuchli, F. H. L. Essler, and F. Mila, Phys. Rev. B **83**, 184433 (2011).
[13] Z.-X. Liu, Y. Zhou, H.-H. Tu, X.-G. Wen, and T.-K. Ng, Phys. Rev. B **85**, 195144 (2012).
[14] F. P. Onufrieva, Zh. Eksp. Teor. Fiz. **89**, 2270 (1985) [Sov. Phys. JETP **62**, 1311 (1985)].
[15] A. Läuchli, F. Mila, and K. Penc, Phys. Rev. Lett. **97**, 087205 (2006).
[16] H. Tsunetsugu and M. Arikawa, J. Phys. Soc. Jpn. **75**, 083701 (2006).
[17] H. Tsunetsugu and M. Arikawa, J. Phys.: Condens. Matter **19**, 145248 (2007).
[18] P. Li, G.-M. Zhang, and S.-Q. Shen, Phys. Rev. B **75**, 104420 (2007).
[19] T. A. Tóth, A. M. Läuchli, F. Mila, and K. Penc, Phys. Rev. Lett. **105**, 265301 (2010).
[20] T. A. Tóth, A. M. Läuchli, F. Mila, and K. Penc, Phys. Rev. B **85**, 140403 (2012).
[21] B. A. Ivanov and A. K. Kolezhuk, Phys. Rev. B **68**, 052401 (2003).
[22] N. Papanicolaou, Nucl. Phys. B **305**, 367 (1988).
[23] V. M. Matveev, Zh. Eksp. Teor. Fiz. **65**, 1626 (1974) [Sov. Phys. JETP **38**, 813 (1974)].
[24] A. Joshi, M. Ma, F. Mila, D. N. Shi, and F. C. Zhang, Phys. Rev. B **60**, 6584 (1999).
[25] A. V. Chubukov, J. Phys.: Condens. Matter **2**, 1593 (1990).
[26] Y. Zhou, K. Kanoda, and T.-K. Ng, Rev. Mod. Phys. **89**, 025003 (2017).
[27] W.-J. Hu, F. Becca, A. Parola, and S. Sorella, Phys. Rev. B **88**, 060402 (2013).
[28] C.-P. Chou and H.-Y. Chen, Phys. Rev. B **90**, 041106 (2014).
[29] S. Morita, R. Kaneko, and M. Imada, J. Phys. Soc. Jpn. **84**, 024720 (2015).
[30] L. Wang and A. W. Sandvik, Phys. Rev. Lett. **121**, 107202 (2018).
[31] L. Wang, Z.-C. Gu, F. Verstraete, and X.-G. Wen, Phys. Rev. B **94**, 075143 (2016).
[32] R. Haghshenas and D. N. Sheng, Phys. Rev. B **97**, 174408 (2018).

[33] H.-C. Jiang, H. Yao, and L. Balents, Phys. Rev. B **86**, 024424 (2012).
[34] L. Capriotti and S. Sorella, Phys. Rev. Lett. **84**, 3173 (2000).
[35] M. Mambrini, A. Läuchli, D. Poilblanc, and F. Mila, Phys. Rev. B **74**, 144422 (2006).
[36] J.-F. Yu and Y.-J. Kao, Phys. Rev. B **85**, 094407 (2012).
[37] S.-S. Gong, W. Zhu, D. N. Sheng, O. I. Motrunich, and M. P. A. Fisher, Phys. Rev. Lett. **113**, 027201 (2014).
[38] H. Georgi, *Lie Algebras In Particle Physics: From Isospin To Unified Theories*, 2nd ed., Frontiers in Physics (Westview, Boulder, CO, 1999).
[39] S. Sarkar, J. Phys. A **24**, 1137 (1991).
[40] J. Exeter and S. Sarkar, Physica B (Amsterdam) **206-207**, 723 (1995).
[41] I. Affleck, M. Oshikawa, and H. Saleur, J. Phys. A **34**, 1073 (2001).